Dr. Sam Milham, MD, MPH
2318 Gravelly Beach Loop NW
Olympia, WA 98502
360-866-0256
sam.milham@gmail.com

BEFORE THE ARIZONA CORPORATION COMMISSION

COMMISSIONERS
TOM FORESE, CHAIRMAN
BOB BURNS
BOYD DUNN
DOUG LITTLE
ANDY TOBIN

IN THE MATTER OF THE APPLICATION OF ARIZONA PUBLIC SERVICE COMPANY FOR A HEARING TO DETERMINE THE FAIR VALUE OF THE UTILITY PROPERTY OF THE COMPANY FOR RATEMAKING PURPOSES, TO FIX A JUST AND REASONABLE RATE OF RETURN THEREON, TO APPROVE RATE SCHEDULES DESIGNED TO DEVELOP SUCH RETURN.	DOCKET # E-01345A-16-0036 **DIRECT TESTIMONY OF DR. SAM MILHAM, MD, MPH ON BEHALF OF WARREN WOODWARD AND IN OPPOSITION TO THE SETTLEMENT AGREEMENT**
IN THE MATTER OF FUEL AND PURCHASED POWER PROCUREMENT AUDITS FOR ARIZONA PUBLIC SERVICE COMPANY	DOCKET # E-01345A-16-0123

Sam Milham, Witness in the above proceeding on behalf of Intervenor Warren

Woodward, hereby submits his Direct Testimony.

1

TABLE OF CONTENTS

I INTRODUCTION

Q. Please state your name, address, and occupation.

A.   Samuel Milham MD, MPH, 2318 Gravelly Beach Loop NW, Olympia WA 98502.

I am a semi-retired physician-epidemiologist.

Q. What is your professional and educational background?

A.   I have a bachelor of science degree from Union College in Schenectady NY, an

MD degree from Albany Medical College in Albany NY, and a masters of public health

degree from Johns Hopkins University in Baltimore MD. I have worked for health

departments and universities. I have over 100 peer reviewed scientific publications,

many of which deal with the health effects of electromagnetic fields. I have written a

book called *Dirty Electricity*. I have a website: www.sammilham.com with copies of

recent publications and a curriculum vitae which lists all my publications. I have been

consulted by dozens of people concerned about the health effects of their smart meters.

Q. What is the purpose of your direct testimony in these proceedings?

A.   I discuss the effects of Arizona Public Service smart meters on the health of

people residing and working in areas where these devices have been deployed.

Q. Have you testified previously before the Commission?

A.   No.

II. SUMMARY OF DIRECT TESTIMONY

Q. Please summarize your direct testimony.

A.   The APS "smart" meters are electronic devices which replaced the old electro-mechanical analog meters used to measure electric power consumption for billing purposes. The smart meters have circuitry to measure power consumption, and a microwave transmitter to send this information to the utility. The health effects of microwave exposures are well known. All transmitters, including the microwave transmitters in smart meters, operate on direct current (DC). The APS smart meters contain a switching mode power supply (SMPS) which changes the utility 60 Hz alternating current to DC.   I will limit my testimony to the health effects of the electrical pollution (dirty electricity) generated by the smart meter SMPS. The dirty electricity problem is compounded by the utility using the earth as a primary neutral return to the substation.

III DIRECT TESTIMONY

Q. Please describe dirty electricity.

A.   "Dirty electricity" or "dirty power" are terms coined by the electric utilities to describe the electrical pollution consisting of high frequency voltage transients and harmonics riding along on the 50 or 60 Hz wave form and contaminating the electricity delivered to users. Dirty electricity is generated by arcing and sparking, especially brush arcing in generators and electrical motors and any device which interrupts current flow, especially switching mode power supplies. These include computers, battery chargers, cell towers, compact fluorescent lights, variable frequency drives, grid tied solar and

4

wind power, and transmitters including smart meters. Dirty electricity is measured with a Graham/Stetzer meter (G/S meter) also known as a Microsurge II meter (MS II meter), which is plugged into electric outlets (Graham, 2005). This meter displays the average rate of change (dV/dT) of these high frequency voltage transients that exist everywhere on electric power wiring and gives a numerical output in Graham/Stetzer or G/S units. It is possible to short out the dirty electricity in wiring by plugging capacitive filters into electrical outlets.

Here's what dirty electricity looks like on an oscilloscope. The pink tracing is dirty electricity, and shouldn't be there.
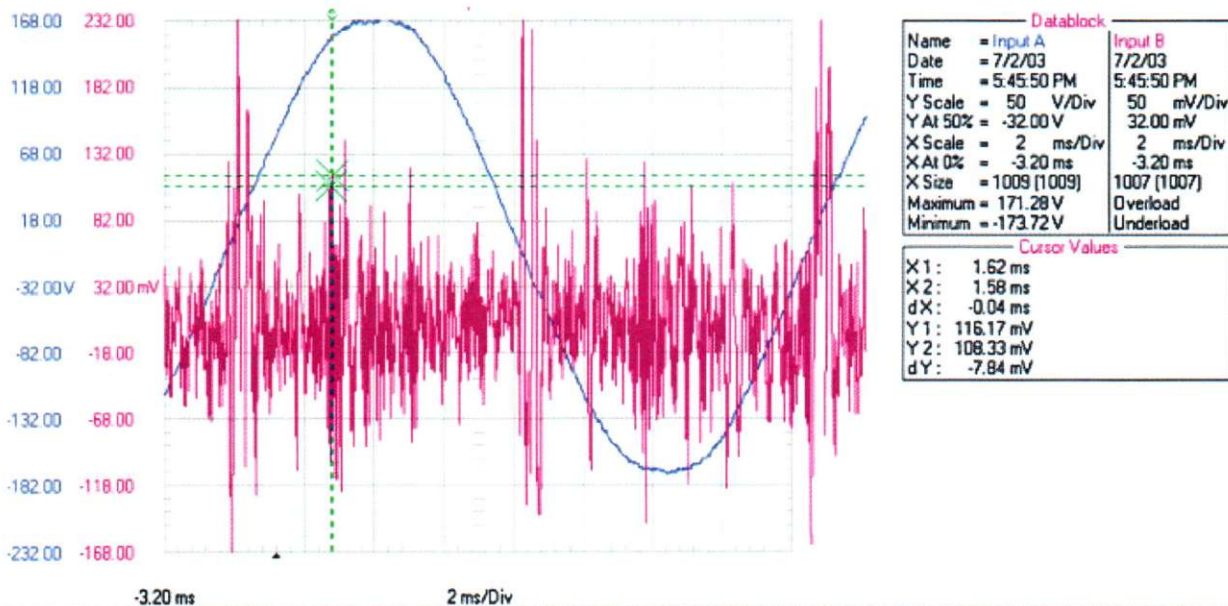
THE WAVEFORM WAS COLLECTED IN ROOM 114 AT THE ELGIN/MILLVILLE MN HIGH SCHOOL. CHANNEL 1 WAS CONNECTED TO THE 120 VAC UTILITY SUPPLIED POWER RECEPTACLE. CHANNEL 2 WAS CONNECTED TO THE SAME POTENTIAL, EXCEPT THROUGH THE GRAHAM UBIQUITOUS FILTER. (REMOVES THE 60 HERTZ) THE AREA BETWEEN THE CURSORS REPRESENTS A FREQUENCY OF 25 KILO HERTZ. A TEACHER WHO PREVIOUSLY OCCUPIED THE ROOM DIED OF BRAIN TUMORS AND THE TEACHER IN THE ADJOINING ROOM DIED OF LUEKEMIA.

**Q. What is the evidence that dirty electricity causes health problems?**

A.   Edison's nine "Jumbo" generators had serious brush arcing problems and commutator wear. This means that from the very beginning of electrification in the U.S. in 1892 and the rest of the world, dirty electricity was being sent out into the grid. In an attempt to control the arcing, he added metallic mercury to the commutators, but this caused illness in his workers. Brushed generators and motors have the same problem today.

The health and mortality effects of electrification and dirty electricity happened so gradually, and on such a wide scale, that they went virtually unnoticed, and the major illnesses that can be attributed to them came to be considered "normal" diseases of modern civilization. By 1900, most cities in the world were electrified, but it took over 50 years for US farms and rural areas to get electricity.

By 1940, more than 90 percent of all the residences in the northeastern United States and California were electrified. By 1940, almost all urban residences in the United States were electrified and urban residents were, therefore, exposed to electromagnetic fields and dirty electricity in their residences and at work, while rural residents were exposed to varying levels of EMFs and dirty electricity, depending on the progress of rural electrification in their states. In 1940, only 28 percent of residences in Mississippi were electrified, while five Southern states had less than 50 percent of residences electrified. Eleven states, mostly in the Northeast, had residential electrification rates above 90 percent. In the highly electrified Northeastern states and in

California, urban and rural residents could have similar levels of EMF exposure, while in states with low levels of residential electrification, there were potentially great differences in EMF exposure between urban and rural residents. It wasn't until 1956 that these differences finally disappeared. What was already known by then, but not appreciated, was that urban death rates were much higher than rural rates for cardiovascular diseases, malignant neoplasms, diabetes and suicide in the 1930 and 1940 United States mortality data. In 1930, urban cancer death rates were 58.8 percent higher than rural cancer death rates.

1940 US white resident crude death rates: percent urban excess
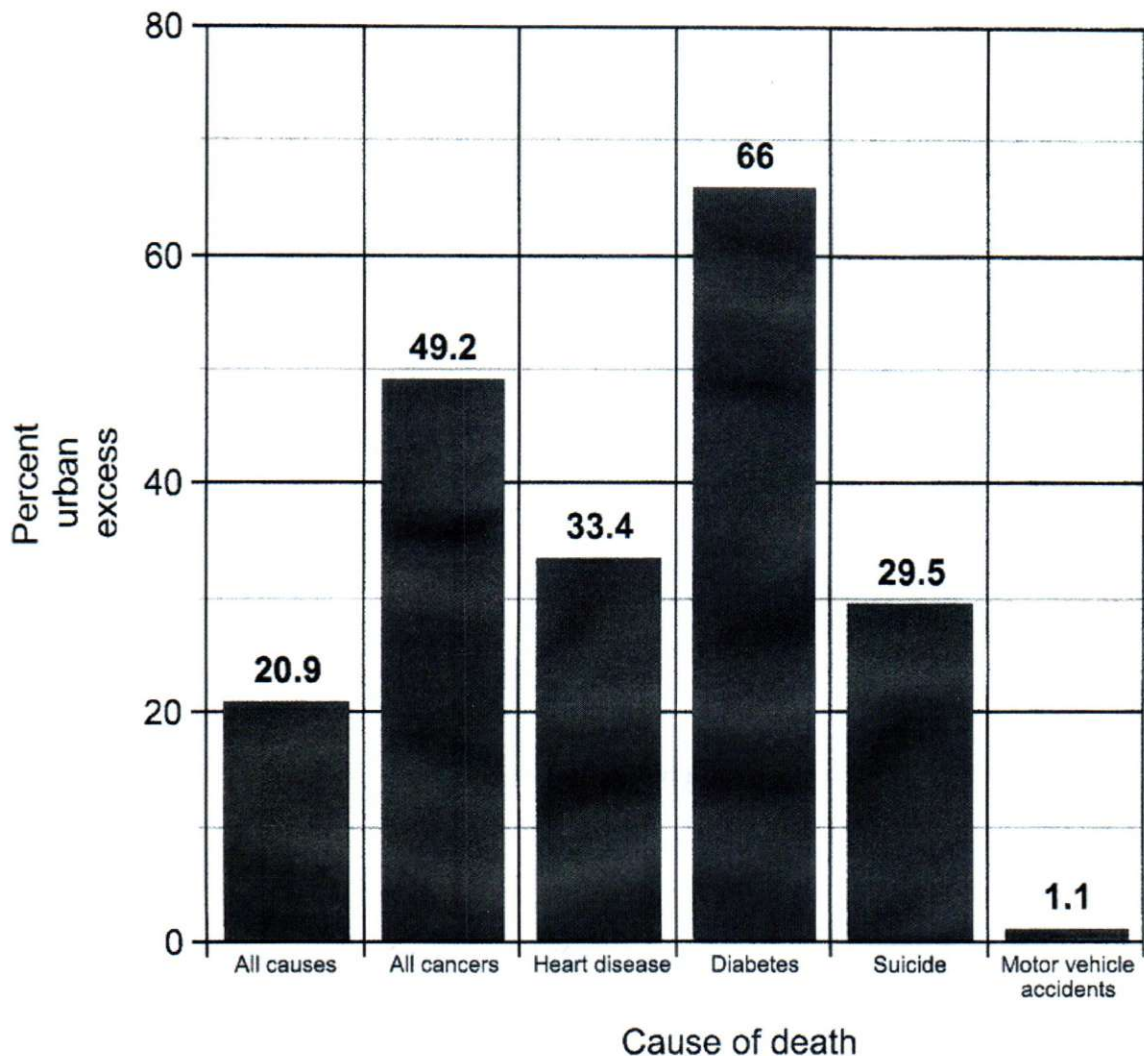
Rural death rates were significantly correlated with the level of residential electric service by state for most of the causes examined. It is difficult to believe that mortality differences of this magnitude could go unexplained for more than seventy years after first being reported, and forty years after they had actually been noticed and commented upon. I suspect that in the early part of the twentieth century, nobody was looking for answers or knew how to properly frame the appropriate broad epidemiologic questions.

By the time electromagnetic field (EMF) epidemiology began in earnest in 1979, the entire population was exposed to EMFs. There was then simply no way to find an unexposed control group; therefore, all studies were potentially biased. Cohort studies, which follow groups of people forward in time, were by then using EMF-exposed population statistics to compute expected values, and case-control studies were comparing more exposed cases to less exposed controls. By way of analogy, the mortality from lung cancer in two-pack-a-day smokers is more than twenty times that of non-smokers, but only three times that of one-pack-a-day smokers. Extending that analogy to EMFs, after 1956, the EMF equivalent of a non-smoker ceased to exist in the United States, with the exception of the small Amish population.

The Old Order Amish (OOA) in North America live without electricity. They have less than half the cancer incidence of the US population (Westman, 2010), and about half the type 2 diabetes prevalence as other US citizens despite having the same body mass index (Hsueh et al, 2000). Cardiovascular disease (Hamman, 1981), Alzheimer's disease (Holder, 1998) and suicide (Kraybill, 1986) are reported to be less common in the OOA. A pediatric group practice in Jasper Indiana which cares for 800 Amish families has not diagnosed a single child with ADHD, and childhood obesity is almost unseen in this population (Ruff, 2005). Remarkably, the life expectancy of the OOA has been about 72 years for the past 300 years for both men and women. In 1900, the life expectancy of U.S. white males was 46.3 years and 48.3 years for white females.

In 2008 I coauthored a study of a cancer cluster in school teachers at a La Quinta, California middle school (see Milham and Morgan, 2008 at my website) which indicated that high frequency voltage transients (also known as dirty electricity), were a potent universal carcinogen with cancer risks over 10.0 and significant dose–response for a number of cancers. They have frequencies between 2 and 100 kHz. These findings are supported by a large cancer incidence study in 200,000 California school employees which showed that the same cancers and others were in excess in California teachers statewide (Reynolds et al, 1999). Power frequency magnetic fields (60 Hz) measured at the school were low and not related to cancer incidence, while classroom levels of high frequency voltage transients (dirty electricity) measured at the electrical outlets in the classrooms accurately predicted a teacher's cancer risk. These fields are potentially present in all wires carrying electricity and are an important component of ground currents returning to substations. This helped explain the fact that professional and office workers, like the school teachers, have high cancer incidence rates. It also explained why indoor workers had higher malignant melanoma rates, why melanoma occurred on parts of the body which never are exposed to sunlight, and why melanoma rates are increasing while the amount of sunshine reaching earth is stable or decreasing due to air pollution. A number of very different types of cancer had elevated risk in the La Quinta school study, in the California school employees study, and in other teacher studies. The only other carcinogenic agent which acts like this is ionizing radiation.

The 2008 study at the La Quinta, California middle school was followed by a study at Vista del Monte elementary school in North Palm Springs, California. This school, like many others had a cell phone tower on campus within 40 feet of a classroom wing. The teachers at this school reported a cancer cluster in the office and teaching staff, and hyperactivity in students in certain classrooms. The entire school had very high dirty electricity readings from the inverter or SPMS in the cell tower. Their dirty electricity levels were higher than those at the La Quinta school. The Vista del Monte G/S readings averaged 1,300 compared to 750 at La Quinta. Fifty G/S units make some people ill. The cancers (twelve cancers, including six female breast cancers among seventy-five personnel employed at the school since 1990) were over-represented in the wing of the school closest to the cell tower, and the G/S readings were highest in the classrooms closest to the cell tower base. At the same stage of the investigation, La Quinta school had eleven cancers in 137 teachers. A fourth grade teacher complained that her students were hyperactive and un-teachable. The outlets in her room measured over 5,000 Graham/Stetzer units. On a Friday afternoon after school, I reduced the measured dirty electricity in the wiring from over 5,000 to less than 50 Graham/Stetzer units with five plug-in filters from Stetzer Electric. With no change in either cell tower radiation or the lighting, the teacher reported an immediate dramatic improvement in student behavior in the following week. They were calmer, paid more attention and were teachable all week except for Wednesday when they spent part of the day in the library.

Later, the teacher told me that she could change the behavior of the children by removing and reinserting the filters. The change took between 30 and 45 minutes. This young teacher also became the thirteenth cancer case in this small teachers' cohort. Filtering the wiring of schools, homes and offices to short out dirty electricity can make dramatic differences in health.

Cell tower transmitters like all transmitters, operate on direct current. They also use the DC to charge their back-up batteries. The utility 60 Hz AC is changed to DC by a switching power supply which generates dirty electricity which contaminates the grid. People who are concerned about health issues regarding cell towers focus on the RF emissions, but dirty electricity is another unrecognized important exposure. A Brazilian study (Dode et al, 2011) showed higher cancer rates within 500 meters of the cell tower base and a dose-response with distance from the tower. Since the transmitted RF intensity decays as the square of the distance from the tower, the dirty electricity is the more likely cause of cancer out to 500 meters.

In 2011 the Lancet published a paper (Danaei et al, 2011), listing fasting plasma glucose (FPG) and diabetes prevalence in 199 countries and territories around the world. Islands are over-represented in places with high blood glucose and diabetes prevalence (Milham, 2013 b). Seven of ten of the places with highest FPG in males are small islands, many in Oceania, while only one of the ten places with the lowest FPG are. In 2011, the same group, Global Burden of Metabolic Risk Factors in Chronic Diseases

Collaborating Group, also published a similar analysis of body mass index (obesity) (Finucane MM et al, 2011), with nearly identical results. I believe that the world wide epidemics of diabetes and obesity are both due to exposure to dirty electricity on electric utility wiring coming from generator brush arcing, bad wiring connections and from cell tower switching power supplies. Islands without fuel supplies are likely to import diesel oil to fuel generator sets which generate dirty electricity which rides along on the 50 and 60 Hz transmission frequencies. If the islands of Oceania are cleaned up electrically, it may take a generation to see the effects.

De-Kun Li (Li DK 2011, 2012) has published two important prospective studies showing that magnetic field exposure during pregnancy increases the risk of asthma and obesity in offspring. Asthma and obesity are rare in Amish children. I believe that magnetic fields are a surrogate for dirty electricity in these studies. I think I also know the etiology of the excess suicides, post traumatic stress disorders, and a number of other Gulf War illnesses. About 85 percent of the fuel oil imported into Afghanistan and Iraq is used for air conditioning at a cost of $ 20.2 billion per year (2011 report). The portable diesel-fueled generator sets which power the air conditioners generate dirty electricity. The wiring also can't be very good, because of the reports of increased accidental electrocution in military personnel in Iraq and Afghanistan. Interestingly, Navy and Air Force personnel don't share the recent suicide increase seen in the Army and Marine Corps.

The highest asthma prevalence rate reported is in the population of Tristan da Cunha, a small Atlantic island with six diesel generator sets for electrical power.

For over eighty years, economists have noted a paradoxical improvement in health indices (declining mortality rates and increasing life expectancy) during economic recessions. Mortality rates increase and life expectancy decreases during economic expansions. The title of a paper (Tapia Granados and Ionides, 2008) "The reversal of the relation between economic growth and health progress: Sweden in the 19th 20th centuries" says it all. The expected decline of health indicators with economic recessions and improvement with economic growth in the 19th century Sweden was reversed in the 20th century, giving the counter-intuitive pattern of higher mortality and lower life expectancy in economic expansions and improvement of these indices in recessions. The change or "tipping point" occurred at the end of the 19th century or early in the 20th century when electrification was introduced into Sweden. All 5 of the reversals of annual industrial electric energy use in the U.S. between 1912 and 1970 were accompanied by recessions with lowered GDP, increased unemployment, decreased mortality and increased life expectancy. The mortality improvement between 1931 and 1932 by state in the U.S. strongly favored urban (electrified) areas over rural areas. Rural unemployment is positively correlated with residential electrification percentage by state in 1930. The health effects of economic change are mediated by electrical exposure (Milham, 2013 a). In recessions, the electric motors which turn the wheels of industry are stilled. The

improvement of health indices in Nazi occupied Europe in WW II and in Cuba during their recent economic collapse were not due to caloric restriction, but to lowered EMF and dirty electricity exposure.

Q. How does the dirty electricity from smart meters expose people?

A.   Because it is at the front end of a building's wiring, the dirty electricity from the smart meter's SMPS has a gateway into that building's wiring, and also into the earth via the house ground. The house wiring acts as an antenna and the fields capacitively couple to the body through the air within 6 to 8 feet of the house wiring or extension cords plugged into the outlets. The ground (green screw) in the breaker box is connected to the utility neutral wire for return to the substation. The grounded Wye grid with numerous connections between the neutral and the earth and inadequate neutral wire current carrying capacity, means that most of the return currents travel in the earth for substation return. This violates the National Electric Safety Code rules 92 D and 215 B, and most state public utility rules. The dirty electricity in the earth makes cows ill and gets into homes thorough conductive water, gas and sewer pipes, utility electric service, and through the foundation rebar in homes built on a concrete slab.

Smart metered neighborhoods have higher dirty electricity levels in the earth. It is possible to get smart meter wave forms in homes without a smart meter and with the electrical service shut off.

Q. How do you think dirty electricity causes health problems?

A.   We are electrochemical soup at the cellular and organ level. Think of ECG (electrocardiogram), EEG (electroencephalogram), and EMG (electromyogram). We evolved in a complex EMF environment with an interplay of natural terrestrial and extra-terrestrial EMF sources from solar activity, cosmic rays, and geomagnetic activity. I believe that our evolutionary balance, developed over the millennia, has been severely disturbed and disrupted by man-made EMFs. I believe that man-made EMFs, especially dirty electricity, are chronic stressors and are responsible for many of the disease patterns of electrified populations. The dramatic differences in mortality in 1940 U.S. data between electrified urban areas and non-electrified rural areas is reported in detail in a 2010 paper (Milham, 2010).

The inescapable conclusion of these findings is that the twentieth century epidemic of the so-called diseases of civilization, including cardiovascular disease, cancer, diabetes and also suicide, was caused by electrification, especially dirty electricity, and the unique biological responses we have to it. A large proportion of these diseases may therefore be preventable.

Q. Can you provide studies that show nerve disruption caused by the same kilohertz frequencies that are generated by APS's smart meters?

A.   Yes. In Exhibit A I have provided a good sampling of abstracts that address those particular frequencies. I have highlighted some of the salient language.

Q. Is there any government funded science or professional institutes that

acknowledge biological affects from current absorbed by human body?

A.   Yes. In Exhibit B I have provided one such example, a study by the Electric Power Research Institute, and it quotes from the National Institute of Environmental Health Sciences (NIEHS) as saying that at a certain level of contact current (which happens to be similar to the exposure a person would have when sleeping next to a wall with a smart meter on the other side) there are "biological effects relevant to cancer."

> In addition to these relative aspects of dose, the absolute (as well as modest) level of contact current modeled (18 μA) produces average electric fields in tissue along its path that exceed 1 mV/m. At and above this level, the NIEHS Working Group [1998] accepts that biological effects relevant to cancer have been reported in ``numerous well-programmed studies". The effects the Working Group cites are ``increased cell proliferation, disruption of signal transduction pathways, and inhibition of differentiation". The NIEHS endorses this conclusion in its final EMF RAPID report [1999].

Q. Does the human body absorb frequencies at the same rate?

A. No, frequencies over 1.7 kHz are absorbed much easier than the 60 Hertz supplied by the utility. At 60 Hertz, the total body impedance is over 3,000 ohms. At 1.7 kHz, the impedance of the skin drops to 500 ohms and continues to drop as frequency increases. At 100 kHz, the impedance is approximately 435 ohms. In layman's terms this means that at high frequencies (over 1.7 kHz) this energy goes internal to the human body. For more information, see the excerpt of the reference book, *Electrical Stimulation and Electropathology,* by J. Patrick Reilly at Exhibit C.

IV CONCLUSION

Q. **DO YOU HAVE ANY CONCLUDING REMARKS?**

A.   Yes. It is my professional opinion that smart meters are a public health hazard.

V REFERENCES

Dirty Electricity by Milham, S. IUniverse 2010, 2012. Available from Amazon, Barnes and Noble.

www.sammilham.com. Recent papers.

Armstrong B, Theriault G, Guenel P, Deadman J, Goldberg M, Heroux P. Association between exposure to pulsed electromagnetic fields and cancer in electric utility workers in Quebec, Canada, and France. Am J Epidemiol (1994). **140** (9) 805–820.

Buchner K, Eger H Changes of clinically important neurotransmitters under the influence of modulated RF fields – a long-term study under real-life conditions. Umwelt-Medizin-Gesellschaft. *(2011)*. **24** 1: 44–57(Original in German)

Danaei, G., Finucane, M. M., Lu, Y., et al. National, regional, and global trends in fasting plasma glucose and diabetes prevalence since 1980: Systematic analysis of health examination surveys and epidemiological studies with 370 countries and 2.7 million participants. Lancet. (2011). **378**: 31–40.

Dode AC et al. Mortality by neoplasia and cellular telephone base stations in the Belo

Dode AC et al. Mortality by neoplasia and cellular telephone base stations in the Belo Horizonte municipality, Minas Gerais state, Brazil. Sci Total Environment: (2011).05.051.

Finucane, M. M., Stevens, G. A., Cowan, M. J., et al.. National, regional, and global trends in body-mass-index since 1980: Systematic analysis of health examination surveys and epidemiological studies with 960 country-years countries and 9.1 million participants. Lancet (2011) **377**:557–567.

Graham MH.. Circuit for Measurement of Electrical Pollution on Power Line. United States Patent 6,914,435 B2 (2005).

Hamman RF, Barancik JL, Lillienfeld AM. Patterns of mortality in the Old Order

Amish. Background and major causes of death. Am J Epidemiol. (1981) **114** 6: 845–861.

Havas M, Stetzer D. (2004). Dirty electricity and electrical hypersensitivity: Five case studies. World Health Organization Workshop on Electrical Hypersensitivity. 25–26 October, Prague, Czech Republic, available online at: http://www.stetzerelectric.com/filters/research/ havas_stetzer_who04.pdf

Havas M, Collings D, Wind Turbines Make Waves: Why Some Residents Near Wind Turbines Become Ill. Bulletin of Science, Technology & Society (2011) XX(X) 1–13.

Holder J, Warren AC. Prevalence of Alzheimer's disease and apolipoprotein E allele frequencies in the Old Order Amish. J Neuropsychiatry Clin Neurosci. (1998). **10** 1: 100–102.

Hsueh, W. C., Mitchell, B. D., Aburomia, R.. Diabetes in the old order Amish: Characterization and heritability analysis of the Amish family diabetes Study. Diabetes Care. (2000) **23**:595–601.

Kraybill DB, Hostetler JA, Shaw DG. Suicide patterns in a religious subculture: the Old Order Amish. J Moral Soc Stud. (1986) 1:249–262.

Li, D. K., Chen, H., Odouli, R. Maternal exposure to magnetic fields during pregnancy in relation to the risk of asthma in offspring. Arch. Pediatr. Adolesc. Med. (2011) **165**:945–950.

Li, D. K., Ferber, J., Odouli, R. et al. Prospective study of In-utero exposure to magnetic fields and the risk of childhood obesity. Sci. Rep. (2012).   doi:10.1038/srep00540.

Milham S, Ossiander EM. Historical evidence that residential electrification caused the emergence of the childhood leukemia peak. Med Hypotheses (2001); **56** (3):290–5.

Milham S, Morgan LL. A new electromagnetic field exposure metric: high frequency voltage transients associated with increased cancer incidence in teachers in a California school.

Am J Ind Med; (2008) **51**(8):579–86.

Milham, S.: Historical evidence that electrification caused the 20th century epidemic of diseases of civilization." *Medical Hypotheses* (2010) **74**, no. 2 337–345.

Milham S,. Hypothesis: the reversal of the relation between economic growth and health progress in Sweden in the nineteenth and twentieth centuries was caused by electrification. Electromagn Biol Med, (2013 a) Early Online: 1–4.

Milham S, Evidence that dirty electricity is causing the worldwide epidemics of obesity and diabetes. Electromagn Biol Med, (2013 b) Early Online: 1–4.

Milham S, Stetzer D. Dirty electricity, chronic stress, neurotransmitters and disease Electromagn Biol Med. (2013) Jan 16. [Epub ahead of print]

Reynolds P, Elkin EP, Layefsky ME, Lee JM. Cancer in California school employees.Am J Ind Med (1999); 36:271.

Ruff, M.E. (2006). Available from:
http://www.additudemag.com/adhd/article/1546.html.

Tapia Granados, J. A., Ionides, E. L., The reversal of the relation between economic growth and health progress: Sweden in the nineteenth and twentieth centuries. J. Health Econ. (2008). **27**: 544–563.

Wertheimer N, Leeper E.. Electrical wiring configurations and childhood cancer. Am J Epidemiol (1979) **109**(3):273–284.

Westman, J. A., Ferketich, K. A., Kauffman, R. M., et al. Low cancer incidence rates in Ohio Amish. Cancer Causes Control. (2010). **21**: 69–75

Respectfully submitted on this 3rd day of April, 2017

Samuel Milham M.D., M.P.H.

Samuel Milham MD, MPH
2318 Gravelly Beach Loop NW
Olympia WA, 98502

Proof of Service

Original and 13 copies of the foregoing hand delivered on this 3rd day of April, 2017 to:

Arizona Corporation Commission
Docket Control Center
1200 W. Washington
Phoenix, AZ 85007

Copies of the foregoing mailed/e-mailed this 3rd day of April, 2017 to:

The Docket Service List

By,

Warren Woodward
200 Sierra Rd.
Sedona, AZ 86336

EXHIBIT A

PubMed

Format: Abstract

Nerve conduction block utilising high-frequency alternating current.

Kilgore KL[1], Bhadra N.

Author information

Abstract

High-frequency alternating current (AC) waveforms have been shown to produce a quickly reversible nerve block in animal models, but the parameters and mechanism of this block are not well understood. A frog sciatic nerve/gastrocnemius muscle preparation was used to examine the parameters for nerve conduction block in vivo, and a computer simulation of the nerve membrane was used to identify the mechanism for block. The results indicated that a 100% block of motor activity can be accomplished with a variety of waveform parameters, including sinusoidal and rectangular waveforms at frequencies from 2 kHz to 20 kHz. A complete and reversible block was achieved in 34 out of 34 nerve preparations tested. The most efficient waveform for conduction block was a 3-5 kHz constant-current biphasic sinusoid, where block could be achieved with stimulus levels as low as 0.01 microCphase(-1). It was demonstrated that the block was not produced indirectly through fatigue. Computer simulation of high-frequency AC demonstrated a steady-state depolarisation of the nerve membrane, and it is hypothesised that the conduction block was due to this tonic depolarisation. The precise relationship between the steady-state depolarisation and the conduction block requires further analysis. The results of this study demonstrated that high-frequency AC can be used to produce a fast-acting, and quickly reversible nerve conduction block that may have multiple applications in the treatment of unwanted neural activity.

PMID: 15191086

[Indexed for MEDLINE]

Publication type, MeSH terms, Grant support

p.23

Blocking central pathways in the primate motor system using high-frequency sinusoidal current

Karen M. Fisher,[1] Ngalla E. Jillani,[2] George O. Oluoch,[2] and Stuart N. Baker[1]

[1]Institute of Neuroscience, Medical School, University of Newcastle upon Tyne, Newcastle upon Tyne, United Kingdom; and
[2]Institute of Primate Research, National Museums of Kenya, Karen, Nairobi, Kenya
Corresponding author.
Address for reprint requests and other correspondence: S. N. Baker, Institute of Neuroscience, Henry Wellcome Bldg., Medical School, Univ. of Newcastle upon Tyne, Framlington Place, Newcastle upon Tyne NE2 4HH, UK (e-mail: stuart.baker@ncl.ac.uk).

This article has been cited by other articles in PMC.

Abstract

Go to:

Electrical stimulation with high-frequency (2–10 kHz) sinusoidal currents has previously been shown to produce a transient and complete nerve block in the peripheral nervous system. Modeling and in vitro studies suggest that this is due to a prolonged local depolarization across a broad section of membrane underlying the blocking electrode. Previous work has used cuff electrodes wrapped around the peripheral nerve to deliver the blocking stimulus. We extended this technique to central motor pathways, using a single metal microelectrode to deliver focal sinusoidal currents to the corticospinal tract at the cervical spinal cord in anesthetized adult baboons. The extent of conduction block was assessed by stimulating a second electrode caudal to the blocking site and recording the antidromic field potential over contralateral primary motor cortex. The maximal block achieved was 99.6%, similar to findings of previous work in peripheral fibers, and the optimal frequency for blocking was 2 kHz. Block had a rapid onset, being complete as soon as the transient activation associated with the start of the sinusoidal current was over. High-frequency block was also successfully applied to the pyramidal tract at the medulla, ascending sensory pathways in the dorsal columns, and the descending systems of the medial longitudinal fasciculus. High-frequency sinusoidal stimulation produces transient, reversible lesions in specific target locations and therefore could be a useful alternative to permanent tissue transection in some experimental paradigms. It also could help to control or prevent some of the hyperactivity associated with chronic neurological disorders.

Keywords: corticospinal, high-frequency block

MANY EXPERIMENTAL AND CLINICAL applications require the control of neural activity. Electrical stimulation is capable of increasing the overall level of activity as well as eliciting action potentials in the stimulated elements at times precisely defined in the submillisecond range. However, in some cases it also can be important to reduce or abolish activity in a chosen pathway. Clinically, this could ameliorate symptoms caused by pathological over activity (e.g., spasticity); experimentally, it allows measurement of responses in which contributions from the blocked pathway have been excluded.

p. 24

Format: Abstract

High-frequency nerve conduction block.

Bhadra N[1], Kilgore KL.

Author information

1   Department of Biomedical Engineering, Case Western Reserve University, Cleveland, OH, USA.

Abstract

High frequency alternating current waveforms have been shown to produce a rapidly reversible nerve block in animal models, but the parameters and mechanism of this block are not well understood. A frog sciatic nerve/gastrocnemius muscle preparation was used to examine the parameters for nerve conduction block in vivo. A complete and reversible nerve block was achieved in all preparations. The results indicate that a 100% block of motor activity can be accomplished with a variety of waveform parameters, including sinusoidal and rectangular waveforms at frequencies from 2 kHz to 20 kHz. The most efficient waveform for conduction block was a 3-5 kHz constant-current biphasic sinusoid. It was demonstrated that the block is not produced indirectly through fatigue.

LinkOut - more resources

PubMed Commons

PubMed Commons home

0 comments

How to join PubMed Commons

P. 25

PubMed

Format: Abstract

Full text links

◆IEEE FULL TEXT PDF

High frequency mammalian nerve conduction block: simulations and experiments.

Kilgore KL[1], Bhadra N.

Author information

Abstract

High frequency alternating current (HFAC) sinusoidal waveforms can block conduction in mammalian peripheral nerves. A nerve simulation software package was used to simulate HFAC conduction block in a mammalian axon model. Eight axon diameters from 7.3 microm to 16 microm were tested using sinusoidal waveforms between 1 kHz to 40 kHz. Block was obtained between 3 kHz to 40 kHz and the current threshold for block increased linearly with frequency above 10 kHz. Conduction block was also obtained for all axon diameters, and the block threshold varied inversely with diameter. Upon initiation, the HFAC waveform produced one or more action potentials. These simulation results closely parallel previous experimental results of high frequency motor block of the rat sciatic nerve. During steady state HFAC block, the axons showed a depolarization of multiple nodes, suggesting a possible depolarization mechanism for HFAC conduction block.

Publication types, MeSH terms, Grant support

LinkOut - more resources

PubMed Commons   PubMed Commons home

P. 26
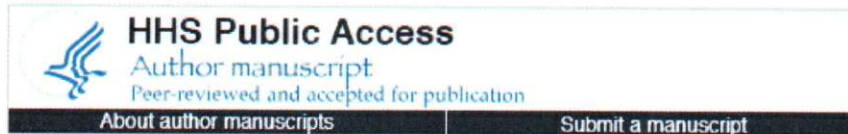
High frequency electrical conduction block of the pudendal nerve

Narendra Bhadra,[1,2] Niloy Bhadra,[1] Kevin Kilgore,[1,4,5] and Kenneth J Gustafson[1,3,4]

[1]Department of Biomedical Engineering, Case Western Reserve University, 10900 Euclid Avenue, Wickenden, Cleveland OH 44106-7207, USA

[2]Department of Orthopaedics, Case Western Reserve University, 10900 Euclid Avenue, Wickenden, Cleveland, OH 44106-7207, USA

[3]Department of Urology, Case Western Reserve University, 10900 Euclid Avenue, Wickenden, Cleveland, OH 44106-7207, USA

[4]Louis Stokes Cleveland Department of Veterans Affairs Medical Center, Cleveland, OH, USA

[5]Department of Orthopaedics, MetroHealth Medical Center, Cleveland OH, USA

Email: kenneth.gustafson@case.edu

Abstract

Go to:

A reversible electrical block of the pudendal nerves may provide a valuable method for restoration of urinary voiding in individuals with bladder–sphincter dyssynergia. This study quantified the stimulus parameters and effectiveness of high frequency (HFAC) sinusoidal waveforms on the pudendal nerves to produce block of the external urethral sphincter (EUS). A proximal electrode on the pudendal nerve after its exit from the sciatic notch was used to apply low frequency stimuli to evoke EUS contractions. HFAC at frequencies from 1 to 30 kHz with amplitudes from 1 to 10 V were applied through a conforming tripolar nerve cuff electrode implanted distally. Sphincter responses were recorded with a catheter mounted micro-transducer. A fast onset and reversible motor block was obtained over this range of frequencies. The HFAC block showed three phases: a high onset response, often a period of repetitive firing and usually a steady state of complete or partial block. A complete EUS block was obtained in all animals. The block thresholds showed a linear relationship with frequency. HFAC pudendal nerve stimulation effectively produced a quickly reversible block of evoked urethral sphincter contractions. The HFAC pudendal block could be a valuable tool in the rehabilitation of bladder–sphincter dyssynergia.

1. Introduction

Go to:

During normal micturition, voiding occurs by synchronized bladder contraction and urethral sphincter relaxation. Spinal cord injury and other neurological disorders can result in detrusor-sphincter dyssynergia (DSD), where bladder and urethral contractions become uncoordinated [1]. DSD can result in significant medical complications such as urinary tract infections, autonomic dysreflexia and renal failure. An efficient and quickly reversible means to block the pudendal nerve and reduce urethral sphincter contractions would provide an effective tool for restoration of urinary voiding in individuals with DSD.

Nerve activation in applications for functional electrical stimulation is usually restricted to frequencies below 50 Hz. Frequencies above 100 Hz have been termed 'high frequency' by various investigators [2, 3]. Such frequencies have often been reported to result in the failure of evoked neural responses [4, 5]. The blocking effects of high frequency alternating current (HFAC) waveforms have been variously reported since 1939 [6].

P. 27

PubMed

Post-stimulation block of frog sciatic nerve by high-frequency (kHz) biphasic stimulation.

Yang G[1,2], Xiao Z[1,3], Wang J[1], Shen B[1], Roppolo JR[4], de Groat WC[4], Tai C[5,6].

Author information

1   Department of Urology, University of Pittsburgh, 700 Kaufmann Building, Pittsburgh, PA, 15213, USA.
2   Department of Biomedical Engineering, Beijing Jiaotong University, Beijing, China.
3   Department of Urology, The Second Hospital, Shandong University, Jinan, China.
4   Department of Pharmacology and Chemical Biology, University of Pittsburgh, Pittsburgh, PA, USA.
5   Department of Urology, University of Pittsburgh, 700 Kaufmann Building, Pittsburgh, PA, 15213, USA. cftai@pitt.edu.
6   Department of Pharmacology and Chemical Biology, University of Pittsburgh, Pittsburgh, PA, USA. cftai@pitt.edu.

Abstract

This study determined if high-frequency biphasic stimulation can induce nerve conduction block that persists after the stimulation is terminated, i.e., post-stimulation block. The frog sciatic nerve-muscle preparation was used in the study. Muscle contraction force induced by low-frequency (0.5 Hz) nerve stimulation was recorded to indicate the occurrence and recovery of nerve block induced by the high-frequency (5 or 10 kHz) biphasic stimulation. Nerve block was observed during high-frequency stimulation and after termination of the stimulation. The recovery from post-stimulation block occurred in two distinct phases. During the first phase, the complete block induced during high-frequency stimulation was maintained. The average maximal duration for the first phase was 107 ± 50 s. During the second phase, the block gradually or abruptly reversed. The duration of both first and second phases was dependent on stimulation intensity and duration but not frequency. Stimulation of higher intensity (1.4-2 times block threshold) and longer duration (5 min) produced the longest period (249 ± 58 s) for a complete recovery. Post-stimulation block can be induced by high-frequency biphasic stimulation, which is important for future investigations of the blocking mechanisms and for optimizing the stimulation parameters or protocols in clinical applications.

KEYWORDS: Block; Frog; High-frequency; Nerve; Stimulation

P. 28
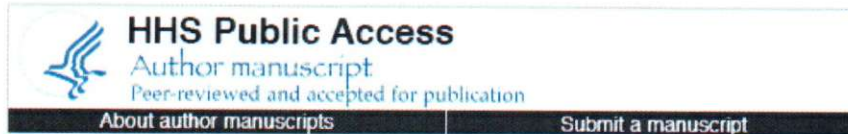
Frequency and amplitude transitioned waveforms mitigate the onset response in high frequency nerve block

Meana Gerges,[2] Emily L. Foldes,[1,2] D. Michael Ackermann,[1] Narendra Bhadra,[1,3] Niloy Bhadra,[1,2] and Kevin L. Kilgore[1,2,3]

[1]Case Western Reserve University, Cleveland, OH, USA
[2]MetroHealth Medical Center, Cleveland, OH, USA
[3]Louis Stokes VA Medical Center, Cleveland, OH, USA

Corresponding Author: Dr. Niloy Bhadra, Hamman 601, MetroHealth Medical Center, 2500 MetroHealth Drive, Cleveland, Ohio, USA, 44109. Email: nxb26@case.edu, Phone: 216 778 3802

The publisher's final edited version of this article is available at J Neural Eng

See other articles in PMC that cite the published article.

Abstract

High frequency alternating currents (HFAC) have proven to be a reversible and rapid method of blocking peripheral nerve conduction, holding promise for treatment of disorders associated with undesirable neuronal activity. The delivery of HFAC is characterized by a transient period of neural firing at its inception, termed the "onset response". The onset response is minimized for higher frequencies and higher amplitudes, but requires larger currents. However, complete block can be maintained at lower frequencies and amplitudes, using lower currents. In this in-vivo study on whole mammalian peripheral nerves, we demonstrate a method to minimize the onset response by initiating the block using a stimulation paradigm with a high frequency and large amplitude, and then transitioning to a low frequency and low amplitude waveform, reducing the currents required to maintain the conduction block. In five of six animals it was possible to transition from a 30 kHz to a 10 kHz waveform without inducing any transient neural firing. The minimum transition time was 0.03 sec. Transition activity was minimized or eliminated with longer transition times. The results of this study show that this method is feasible for achieving a nerve block with minimal onset responses and current amplitude requirements.

Keywords: High frequency nerve block, functional electrical stimulation, onset response, in-vivo model

INTRODUCTION

The delivery of high frequency alternating currents (HFAC) has proven to be a reversible and rapid method of blocking peripheral nerve conduction [1–8]. HFAC in the frequency range of 1 – 40 kHz [9–10], delivered through a cuff electrode in direct contact with a peripheral nerve, has been shown to reversibly block the propagation of action potentials [7, 11]. The typical HFAC amplitude ranges between 1 – 10 V (peak to peak) in order to achieve complete block and is dependent on the frequency used and the electrode to nerve interface [8–9]. Block is established in less than 100 ms [11] and is completely reversible when the HFAC is turned off, as the nerve returns to full conductivity within approximately one second [5, 7–8]. The fast onset of the conduction block and the quick reversibility makes HFAC block appealing for potential clinical uses. Recent studies in rats [8, 12–14], frogs [7], and cats [6, 9, 15] have shown that HFAC is an effective method of blocking peripheral

P. 29
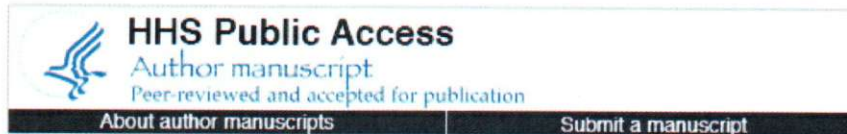
Electrical Conduction Block in Large Nerves: High Frequency Current Delivery in the Nonhuman Primate

D. Michael Ackermann, Jr., Ph.D.,[1,2] Christian Ethier, Ph.D.,[3] Emily L. Foldes, M.S.,[2] Emily R. Oby,[3] Dustin Tyler, Ph.D.,[2] Matt Bauman,[3] Niloy Bhadra, M.D., Ph.D.,[2,1] Lee Miller, Ph.D.,[3] and Kevin L. Kilgore, Ph.D.[1,2,4]

[1]MetroHealth Medical Center, Cleveland, OH, USA

[2]Case Western Reserve University, Cleveland, OH, USA

[3]Northwestern University, Evanston, IL, USA

[4]Louis Stokes Veterans Affairs Medical Center, Cleveland, OH, USA

Corresponding Author: D. Michael Ackermann, Ph.D., Cleveland FES Center, Hamman 601, 2500 MetroHealth Drive, Cleveland, OH 44109, Email: dma18@case.edu

See other articles in PMC that cite the published article.

Abstract

Go to:

Recent studies have made significant progress toward the clinical implementation of high frequency conduction block (HFB) of peripheral nerves. However, these studies were performed in small nerves, and questions remain regarding the nature of HFB in large diameter nerves. This study in nonhuman primates shows reliable conduction block in large diameter nerves (up to 4.1 mm) with relatively low threshold current amplitude and only moderate nerve discharge prior to the onset of block.

Keywords: high frequency alternating current (HFAC), peripheral nerve, conduction block, primate, large diameter

Introduction

Go to:

The delivery of high frequency alternating current (HFAC) to peripheral nerves can produce a reversible conduction block[1]. There is considerable hope that the method may be useful for the clinical treatment of disorders associated with pathological neural activity, such as spasticity or peripherally triggered pain. HFAC delivery has been the focus of several recent studies which have pursued an optimal waveform for delivery, optimal electrode design and a biophysical understanding of the mechanisms of this type of nerve conduction block. The results of these studies demonstrate that high frequency block (HFB) can be established quickly (≤ 1 sec to several seconds)[2,3] and reversed quickly (≤ 1 sec)[2]. The induction of HFB requires the use of a frequency that is at least ~2 kHz[4–7] and a waveform amplitude that is typically 3 V – 10 V (1 mA – 10 mA for current-controlled studies) across preparations[4,6–9]. The minimal waveform amplitude required to induce HFB, the block threshold, is dependent on the waveform frequency[4,6,8,10,11] and geometry of the blocking electrode[12]. When HFAC is first applied to a nerve, it produces an intense volley of activity in the target nerve, the 'onset response,' before inducing block. The magnitude and duration of this onset response are also functions of the waveform frequency[6,10], waveform amplitude[1,6,10,13,14] and electrode geometry[14]. HFB has been successfully demonstrated in a chronic electrode preparation in the cat[6] and likely results, mechanistically, from

P. 30

EXHIBIT B

The Possible Role of Contact Current in Cancer Risk Associated With Residential Magnetic Fields

R. Kavet,[1]* L. E. Zaffanella,[2] J. P. Daigle,[2] and K. L. Ebi[1]

[1]EPRI, Palo Alto, California
[2]Enertech Consultants, Lee, Massachusetts

Residential electrical wiring safety practices in the US result in the possibility of a small voltage (up to a few tenths of a volt) on appliance surfaces with respect to water pipes or other grounded surfaces. This "open circuit voltage" (V_{OC}) will cause "contact current" to flow in a person who touches the appliance and completes an electrical circuit to ground. This paper presents data suggesting that contact current due to V_{OC} is an exposure that may explain the reported associations of residential magnetic fields with childhood leukemia. Our analysis is based on a computer model of a 40 house (single-unit, detached dwelling) neighborhood with electrical service that is representative of US grounding practices. The analysis was motivated by recent research suggesting that the physical location of power lines in the backyard, in contrast to the street, may be relevant to a relationship of power lines with childhood leukemia. In the model, the highest magnetic field levels and V_{OC}s were both associated with backyard lines, and the highest V_{OC}s were also associated with long ground paths in the residence. Across the entire neighborhood, magnetic field exposure was highly correlated with V_{OC} ($r = 0.93$). Dosimetric modeling indicates that, compared to a very high residential level of a uniform horizontal magnetic field (10 µT) or a vertical electric field (100 V/m), a modest level of contact current (~ 18 µA) leads to considerably greater induced electric fields (> 1 mV/m) averaged across tissue, such as bone marrow and heart. The correlation of V_{OC} with magnetic fields in the model, combined with the dose estimates, lead us to conclude that V_{OC} is a potentially important exposure with respect to childhood leukemia risks associated with residential magnetic fields. These findings, nonetheless, may not apply to residential service used in several European countries or to the Scandinavian studies concerned with populations exposed to magnetic fields from overhead transmission lines. Bioelectromagnetics 21:538–553, 2000.
© 2000 Wiley-Liss, Inc.

INTRODUCTION

Background

The question of whether residential exposure to power frequency (50 and 60 Hz) magnetic fields is a risk factor for childhood leukemia remains unresolved [NIEHS Working Group, 1998; NIEHS, 1999]. Early epidemiological studies conducted in Denver and Los Angeles reported associations between electric utility line wiring configurations and childhood leukemia [Wertheimer and Leeper, 1979; London et al., 1991] or all childhood cancer [Savitz et al., 1988], with a suggestion of increased leukemia risk in the latter. As developed initially by Wertheimer and Leeper [1979, 1982] with subsequent refinements by others [Barnes et al., 1989], the wiring configurations were the basis of a categorical exposure surrogate, referred to as the "wire code". The positive relation between wire code and magnetic field [reviewed in Kheifets et al., 1997], as well as suggestive associations between measured fields and relative risk estimates [Savitz et al., 1988; London et al., 1991], appeared consistent with the hypothesis that the residential magnetic field was the causal agent in these studies.

In a recent re-analysis of the Denver and Los Angeles studies, Ebi et al. [1999] report that in both data sets, risk associated with wire code was concentrated in residences served by backyard distribution lines, as opposed to distribution lines in the street. This observation motivated the analysis presented in this paper, which is concerned with (a) the relationship

P. 32

between the physical features of residential electric service and exposures to magnetic fields and currents; (b) the correlation among specific electric and magnetic exposure parameters; and (c) the dosimetric implications of these relationships with respect to childhood leukemia risk. We introduce an exposure called the "open circuit voltage" (V_{OC}), which is a small power frequency voltage (up to a few tenths of a volt) that may appear on electrical equipment. V_{OC} can cause a "contact current" to flow directly into a person in manual contact with the appliance. The findings presented in this paper suggest that contact current due to V_{OC} may be an exposure variable that could hold the key to clarifying the reported associations of power line environments with childhood leukemia. We first review the relevant aspects of residential electrical service.

Residential Electrical Service

The major features of electrical service in US distribution systems are illustrated in Figure 1 and further elaborated in its caption. Electrical service to the residence occurs via the "service drop", which connects the distribution transformer secondary located outside on a utility pole or underground, to the "service panel", where the occupant has access to circuit breakers and/or fuses. The service drop consists of three cables: two 120 volt (V) alternating current (ac) "hot legs", which provide the load currents for lights, appliances, etc., and the neutral, through which current may return to the substation.

For safety purposes, e.g., electric shock and fire prevention, residential electrical wiring in the US provides multiple pathways for current to return to the substation [NESC, 1992]. Under normal conditions, the current returns via both the utility's service drop neutral and an alternative pathway, which in many cases is a conductive residential plumbing line connected to the municipal water main in the street. The connection to the plumbing is established with a "ground wire" bonded electrically to the utility neutral at the service panel and strung at some length to a convenient (exposed) water line. For cases in which conductive water pipes are not available, houses will have driven ground rods to establish a strong alternative ground connection. The amount of current that each pathway takes has an inverse relationship to each pathway's electrical resistance.

The "net load current" is the algebraic sum of the current in the two supply conductors. The "net current" in the utility service drop equals the net load current to the residence minus the current in the service drop neutral. Net current equals the current that flows in the alternative ground pathways, which we refer to

as the "ground current" (see Figure 1). Thus, the service drop to ground wire pathway becomes a magnetic field source in the residence. The source strength depends on the current magnitude and the pathway's geometry. In residences located away from overhead utility distribution or transmission lines, Kavet et al. [1999] report that, compared to other predictor variables, the net service drop current (i.e., the ground current) correlates most strongly with magnetic fields measured in the residence. In communities with conductive water service and water mains, a fraction of ground current generated in one residence may flow to another residence's ground.

Since the ground wire has a resistance, though small, the current flowing in it produces a voltage difference between the service neutral and the plumbing connection. This voltage equals the ground wire current multiplied by the wire's resistance (assuming no additional resistance due to poor bonding at the wire's termini). To prevent shock, electrical appliances have their metallic chassis connected, either through their neutral wire or their third wire, to the utility neutral bonding point in the service panel (Figure 1). Through this connection, the chassis carries the voltage generated in the ground wire, which we refer to as the "open circuit voltage" or V_{OC}. As indicated by the open switch in Load 3 in Figure 1, V_{OC} is present on an appliance even when in the "off" position, so long as it is plugged in.

V_{OC} can serve as a source of contact current into a person who touches the chassis, and, through either the other hand or the feet, completes an electrical circuit back to the house's ground. This circuit is shown schematically in Figure 2. The resistance of the ground wire, R_{GW}, is usually very small (around 0.1 ohm (Ω) for a 30 m length) compared to the resistance in the rest of the contact current pathway, which consists of R_P, the resistance of the individual, in series with R_G, the resistance from the feet back to ground. R_P is on the order of several thousand ohms [Reilly, 1998], but varies depending on skin moisture and other factors; R_G depends on footware, floor material, and housing materials. Thus, since $R_{GW} \ll R_P + R_G$, contact current is essentially equal to V_{OC} divided by the sum of R_P and R_G. If the other hand comes in contact with a water fixture, which is usually at house ground potential, then the contact current would likely take the hand-to-hand route as the path of lower resistance.

Organizations concerned with EMF exposure guidelines [e.g., International Commission on Non-Ionizing Radiation Protection (ICNIRP)] and appliance safety [e.g., Underwriters Laboratories (UL)] have published limits for contact or "leakage"
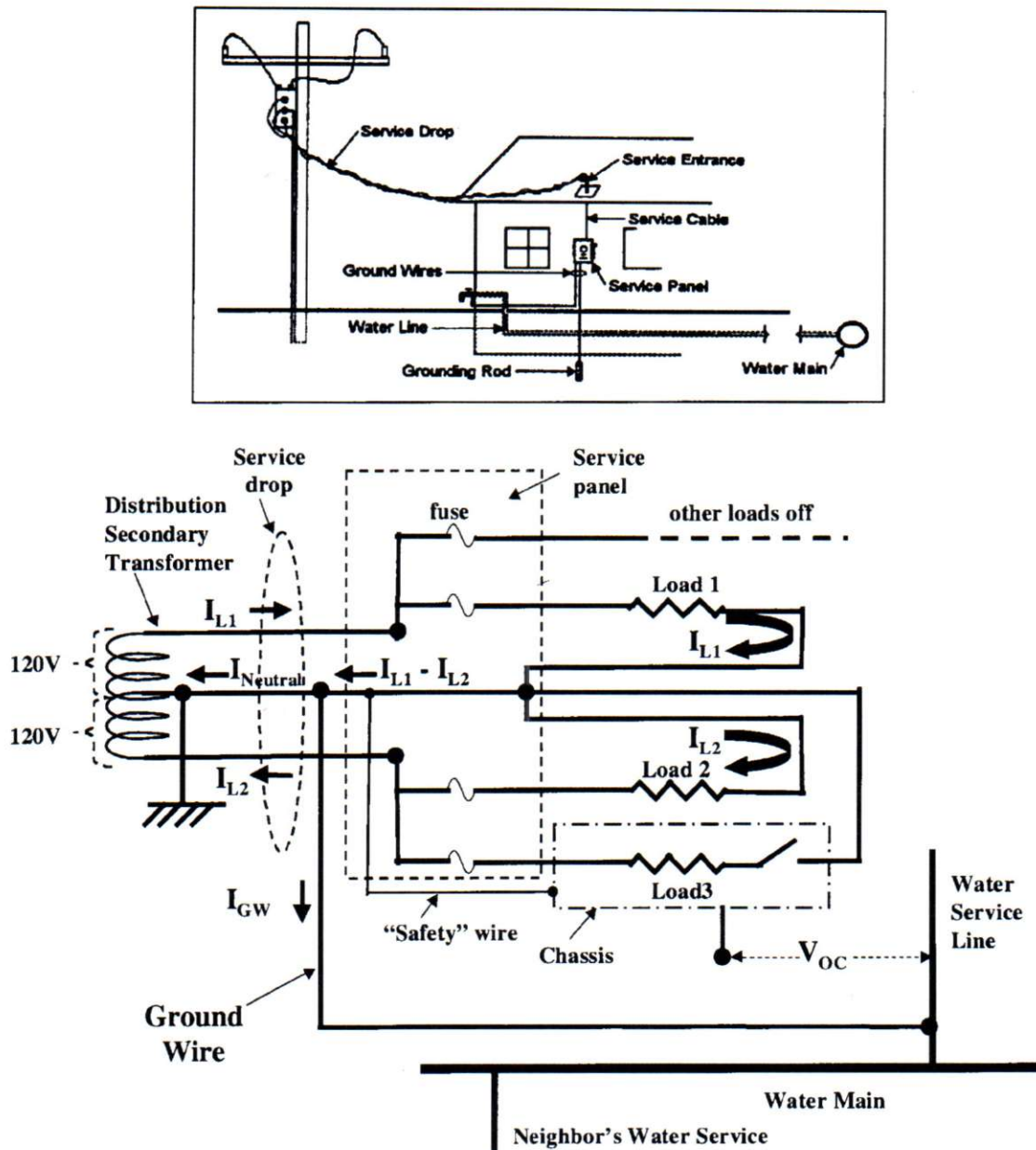
Fig. 1. Residential Electric Service Typical of "Multi-grounded Neutral" Systems used in the US and Origin of Open Circuit Voltage (V_{OC}). Top inset is a "real world" view of electrical service to a single-unit residence. Bottom graphic is a schematic of the electrical relationships in the service and internal wiring. Two 120-V conductors (hot legs) from the distribution secondary transformer, 180 degrees out of phase with each other, supply currents I_1 and I_2 to Load 1 and Load 2, respectively. The center tap of the transformer is grounded at the street pole or underground transformer location. The "net load current" on the service drop is the amount of current returning to the substation at any point in time and, in the figure, equals $I_{L1} - I_{L2}$. Current returns via two basic pathways: (a) the service drop neutral cable or (b) an alternate ground path, which in the figure consists of a ground wire connected to a conductive water line. The net load current equals the sum of the currents in these two pathways, $I_{Neutral} + I_{GW}$. The "net current" in the service drop equals net load current minus the current in the neutral, or $I_{Net} = (I_{L1} - I_{L2}) - I_{Neutral}$. The current in the ground wire, I_{GW}, equals I_{Net}. I_{GW} and I_{Net} are sources of magnetic field in the residence. Because the ground wire has a finite resistance, R_{GW} (not pictured), a voltage is developed across its length equal to $I_{GW} \times R_{GW}$, which we refer to as the open circuit voltage (V_{OC}). Load 3, plugged in but in the off position (open switch), has a safety wire that connects the load's chassis to the service panel neutral. The chassis is, thus, at a voltage V_{OC} with respect to the grounded water system. In this model, V_{OC} represents the largest voltage potentially present prior to contact between a person and an appliance chassis or between a person and metallic structures (e.g., hot water heaters, steam radiators) connected to residential water pipes. Ground currents may be shared among residences.
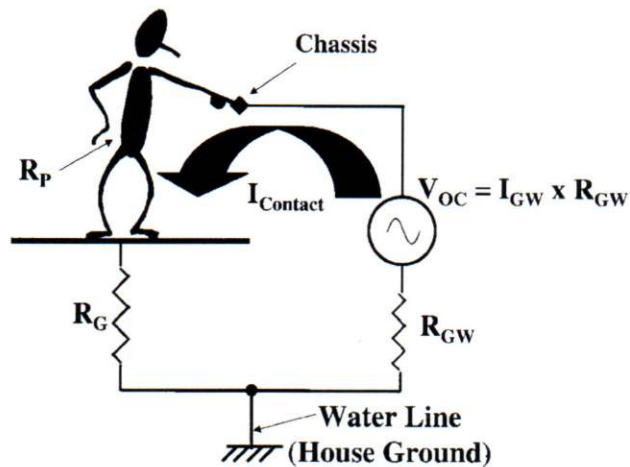
P. 34

Fig. 2. Contact Current. A person contacting a chassis is exposed to V_{OC}, which can drive current into that person, depending on the nature of his/her connection to the chassis and to the ground. Moist extremities decrease a person's electrical skin resistance, while insulating footwear or poorly conductive housing materials will sharply limit current. The figure shows hand-to-feet contact, but if the second hand is in touch with a grounded object, the current will take a hand-to-hand route.

currents. These limits are designed to avert hazardous startle and adverse perceptual effects. Below 2.5 kHz, ICNIRP [1998] specifies 0.5 mA and 1.0 mA contact current limits for the general public and workers, respectively. UL lists 0.5 mA and 0.75 mA as startle limits for portable and fixed appliances, respectively [reviewed in Reilly, 1998]. The National Electric Safety Code [NESC, 1992], which specifies safety practices for overhead transmission line construction and operation, limits to 5 mA steady-state whole body current that may result from electric field induction on large objects (e.g., trucks) in physical contact with a person in the right-of-way of overhead high-voltage transmission lines.

Study Overview

We constructed a computer model of a 40 house neighborhood to address how specific physical features of residential electrical service affect magnetic field and V_{OC} exposures within the residence. The software running the model has been previously validated against measurements taken in a test residence under various grounding conditions [Zaffanella et al., 1997]. The features we examined are line location—backyard or street, relative length of the ground return pathway—short or long, and service line type—overhead or underground. The quantities modeled include the 60 Hz and 180 Hz magnetic fields at the center of each room, the time-weighted-average fields experienced by a child as a result of a day's occupancy of the residence, and the V_{OC}. The neighborhood wiring

follows practices applicable to the US, although we recognize that such practices vary among countries [Rauch et al., 1992]. Despite the stochastic nature of the residential loading imposed on the neighborhood, the model itself is completely deterministic, and the statistical treatment of the data is intended to clarify relationships among exposure and source variables, rather than to achieve inferential support as occurs in population studies.

METHODS

Modeling Software

The modeling software calculates magnetic fields resulting from currents on arbitrary arrays and configurations of electric transmission lines, primary and secondary distribution lines, and ground and neutral return pathways. The program conducts network analyses of ground/neutral currents in neighborhoods based on user-specified residential loads and impedances. Local dipole sources, such as appliances, are not included in the field calculation. As mentioned above, the program has been previously validated against measured fields and known ground currents [Zaffanella et al., 1997].

Modeling Objective

This paper is concerned exclusively with magnetic fields and $V_{OC}s$ resulting from currents in the service drop (i.e., secondary distribution current) and in the ground path (Figure 1). Wertheimer-Leeper wire code categories do not play a role in the model as configured for the analyses here. In fact, for the neighborhood loading used here, primary loads and their return currents had a negligible effect on residential magnetic fields and V_{OC}. However, the neighborhood was provided with a full range of distribution wiring configurations representative of the Wertheimer-Leeper wire code, should further development of the neighborhood (e.g., downstream connections to other load centers) be warranted. The appendices contain a detailed description of the neighborhood's electrical infrastructure.

Neighborhood Description

Briefly, the study neighborhood (Figure 3) consists of four streets containing 40 two-story houses, each 10.7 m by 7.6 m (35×25 ft) with the long dimension parallel to the street. Each house has eight equal-size rooms, four per floor. For each house, the service drop arrives at a corner and then goes to the electrical panel. All houses have copper-pipe water service that provides a conductive ground path to the
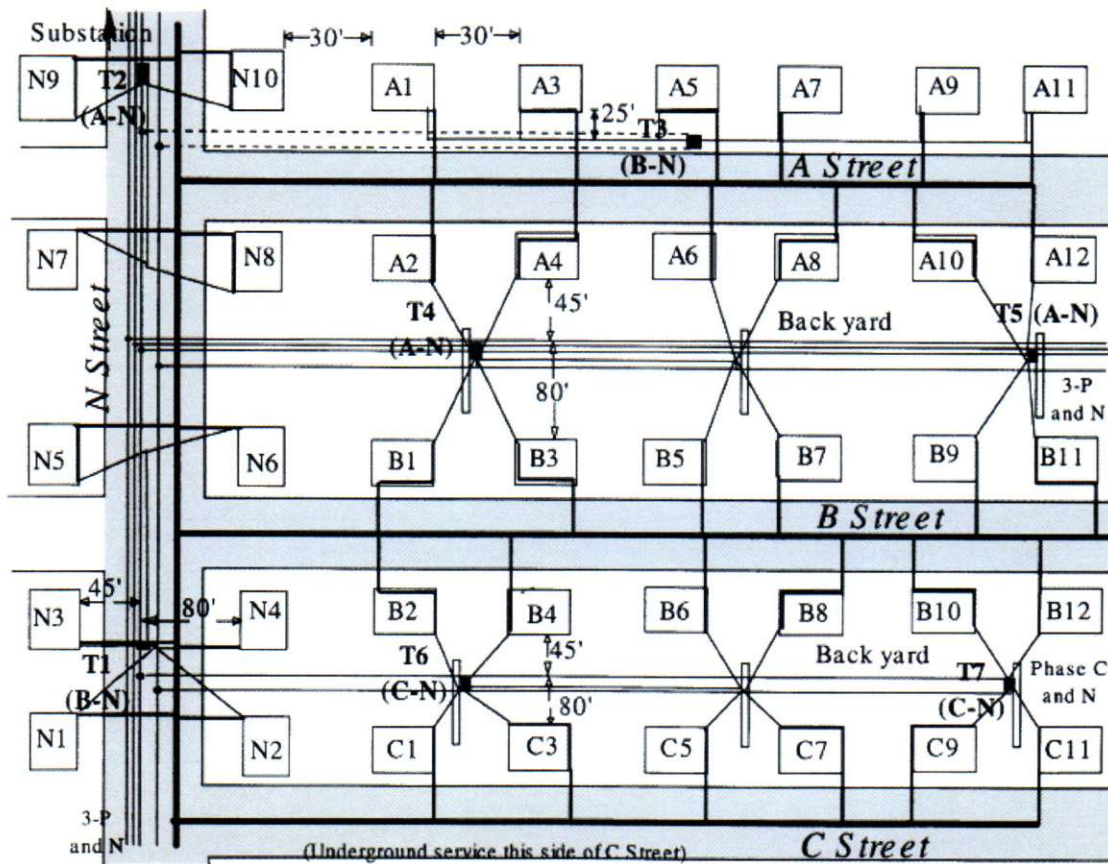
Fig. 3. Model neighborhood (see text and Appendix).

water main. All water mains were located in the middle of the street.

With the exception noted below, all combinations of the following attributes were represented: line location—backyard or street; relative length of the ground return pathway—short or long; and service line type—overhead or underground. Underground lines were not situated in the backyard, as this is a less common feature of residential electric distribution systems. Figure 4 illustrates the "length of ground path" dichotomous variable: Type 1 is the shorter possible path for overhead street lines, overhead backyard lines, and underground street lines (top to bottom in Figure 4); Type 2 is the longer possible path for overhead street lines, overhead backyard lines, and underground street lines (top to bottom in Figure 4).

Loading

As discussed above and shown in Figure 1, the net load is the parameter that defines the electrical load of the house with regard to ground current. The "1,000-home study" [Zaffanella, 1993] developed a database of electrical parameters, including the 24 h statistical distribution of the net load for each house. These data suggested using a net load for each house randomly extracted from a log-normal distribution with a median value of 4.34 ampere (A) and a geometric standard deviation of 1.87. The model was run 100 times, each time with a net load randomly allocated to each house. To account for possible ground current interactions between residences, the sign of the net load was also randomly chosen. The load currents were all at the power frequency of 60 Hz with a 15% third harmonic. The value chosen for the third harmonics corresponded to the average value recorded during the 1000 home survey [Zaffanella, 1993].

RESULTS

General Statistical Description of Sample

The parameters selected for study are listed in Table 1, and their descriptive statistics across the entire neighborhood are shown in Table 2. The variables displayed continuous, smooth distributions, although

P. 36

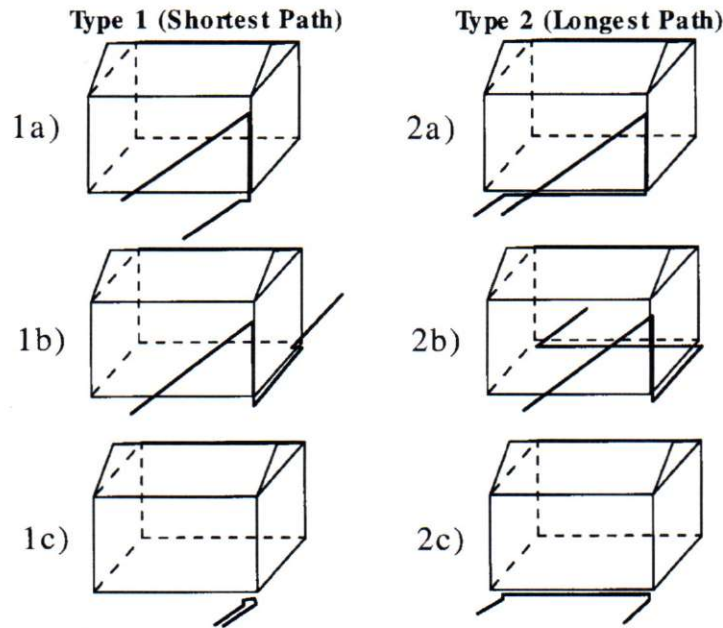**Type 1 (Shortest Path)**   **Type 2 (Longest Path)**

Fig. 4. Net and ground current paths: 1a) Overhead street line, short path; 1b) Overhead backyard line, short path; 1c) Underground street line, short path; 2a) Overhead street line, long path; 2b) Overhead backyard line, long path; 2c) Underground street line, long path.

TABLE 1. Parameters Reported on in Results[a]

Parameter	Description
AvgRoomB	Temporal average of the 60 Hz magnetic field in the center of each room 1 m above the floor averaged across all eight rooms
Avg180HzB	Temporal average of the 180 Hz magnetic field in the center of each room 1 m above the floor averaged across all eight rooms. Typical values of harmonic loads are assumed [Zaffanella, 1993]
AvgPerimB	Temporal average of the magnetic field sampled every 5 m around the house periphery, 1 m from the house, and 1 m off ground
AvgChildB	Temporal average of the field across the entire indoor space, from floor to four feet above the floor. The field is calculated at all points of a three-dimensional grid with one foot (0.305 m) grid size. For each floor of a 10.7 m by 7.6 m (35 × 25 ft) house, there are 4680 calculation points in the "child" space
10%ChildB	The upper 10th percentile value of child's exposure within a house
AvgGC	The temporal average of the current in the residential ground path; same as average net current in the service drop
10%GC	The upper 10th percentile value of GC within a house
$AvgV_{OC}$	Temporal average of the open-circuit voltage between appliance chassis and the water line at the point where it is connected to the conductor that grounds the electric service neutral
$10\%V_{OC}$	The upper 10th percentile value of V_{OC} within a house

[a]Within each residence parameters are calculated for each of 100 loads randomly assigned. Thus, for example, AvgGC for a residence is the ground current averaged over 100 values; 10%GC for a residence is the value exceeded for 10% of the calculations.

most were not normally distributed according to the Shapiro-Wilk test.

Stratification of Sample

By design (see Methods), only the currents in the service secondaries, service neutral, and ground pathways influenced the electrical quantities computed for each residence. Thus, all one-, two-, and three-phase primary lines were collapsed into one "overhead" (OH) category, with the remainder classified as "underground" (UG). The basic geometric differences between OH and UG are evident in Figure 4.

Table 3 shows summary statistics for several key exposure variables, stratified by engineering factors. Visual inspection suggests that the highest field exposure quantities were associated with backyard, overhead lines, the highest ground currents were associated with overhead lines, and the highest $V_{OC}s$ were associated with overhead, backyard lines with long ground paths.

TABLE 2. Descriptive Statistics for Selected Exposure Variables for the Entire Neighborhood Sample ($N=40$ Houses)

Statistic	AvgRoom B (μT)	Avg180Hz B (μT)	AvgPerim B (μT)	AvgChild B (μT)	10%Child B (μT)	AvgGC (A)	10%GC (A)	AvgV$_{OC}$ (mV)	10%V$_{OC}$ (mV)
Mean	0.077	0.014	0.118	0.097	0.169	1.44	2.82	54.4	107.1
SD	0.046	0.009	0.096	0.052	0.103	0.64	1.22	34.2	67.6
Median	0.088	0.016	0.085	0.095	0.169	1.23	2.47	53.2	105.2
Upper 10%	0.135	0.025	0.264	0.177	0.320	2.53	4.79	90.8	187.5
Lower 10%	0.012	0.002	0.011	0.021	0.008	0.79	1.53	10.4	20.0
Shapiro-Wilk P-value	<0.05	<0.01	<0.01	>0.1	>0.3	<0.01	<0.01	<0.05	<0.05

TABLE 3. Summary Statistics for Selected Exposure Measures Broken Down by System Characteristics

Line type	Location	Ground type	N	AvgRoomB (μT) Median	AvgRoomB (μT) Min–Max	AvgChildB (μT) Median	AvgChildB (μT) Min–Max	AvgGC (A) Median	AvgGC (A) Min–Max	AvgV$_{OC}$ (mV) Median	AvgV$_{OC}$ (mV) Min–Max
OH	Backyard	Short	12	1.12	0.12–1.64	1.05	0.61–1.83	1.49	0.88–2.60	52.0	30.7–91.0
OH	Backyard	Long	12	0.99	0.54–1.63	1.12	0.80–2.14	1.09	0.78–2.10	74.5	53.7–144.0
OH	Street	Short	6	0.72	0.41–1.09	0.73	0.34–1.01	2.13	0.98–2.80	20.9	9.6–27.6
OH	Street	Long	4	0.53	0.14–1.03	1.05	0.34–1.42	1.46	0.48–1.98	64.6	21.1–87.7
UG	Street	Short	4	0.10	0.04–0.15	0.17	0.14–0.21	1.01	0.83–1.22	10.0	8.2–12.0
UG	Street	Long	2	—	0.18–0.18	—	0.25–0.40	—	0.51–0.79	—	22.4–35.1

Regression Model

A linear regression model was used to clarify the dependencies between the three factors (line type, location, and ground type) and the nine computed exposure variables:

$$\text{Exposure} = \beta_1 * (\text{Line Type}) + \beta_2 * (\text{Location}) + \beta_3 * (\text{Ground Type}) + \varepsilon$$

The results of the regression analysis are summarized in Table 4. The computed P-values shown cannot be taken too literally because the residual "errors" are not random and because if the number of houses and number of temporal samples were increased, all the P-values would necessarily become smaller. In general, exposure values were increased for residences served by backyard OH lines. Not surprisingly with their lower resistance, short ground paths increased ground current, and the long ground path increased V$_{OC}$.

The results in Table 4 were generally consistent with subgroup models that included OH lines only ($N=34$; Location and Ground Type predictors); backyard lines only ($N=24$; Ground Type predictor only); and street lines only ($N=16$; Line Type and Ground Type predictors).

Correlation of Exposure Variables

Table 5 shows the Pearson correlation among the six average exposure parameters under study. The nonparametric Spearman test produced essentially the same results. The nearly perfect correlation between AvgRoomB and Avg180HzB is not surprising as sources for both exposures and methods for field calculation are tightly linked.

We note a very high correlation ($r = .93$ or about 87% explained variance) between AvgChildB and AvgV$_{OC}$. The correlations between these two parameters and the other exposure variables were relatively weaker. The reasons for this difference are (1) the way AvgChildB was computed, compared to the other field quantities (see Table 1), and (2) the relation between ground current (GC) and both AvgChildB and V$_{OC}$, as compared to the other field quantities. First, AvgChildB was computed across the entire floor space of the residence and thus it controls for asymmetric service and ground wiring patterns among residences. AvgRoomB, which represents the average field from only the center of each house's rooms, does not completely control for asymmetry, nor does AvgPerimB taken at selected points outside the residence.

Second, linear regression allows us to observe that, within both Backyard ($N=24$) and Street ($N=16$) strata, the following model accounts for 100% of the variability in both AvgV$_{OC}$ and AvgChildB (of course, the value of the α coefficients are different for AvgV$_{OC}$ and AvgChildB):

$$\text{AvgV}_{OC} \text{ or AvgChildB} = \alpha_1 * (AvgGC) + \alpha_2 * (\text{Ground Type}) + \alpha_3 * (\text{Ground Type})^* (AvgGC) + \varepsilon$$

P. 38

TABLE 4. Summary Results of Regression Analysis of Full Sample ($N=40$)

Exposure variable	Predictor variables		
	Line type (OH or UG)	Location (Backyard or Street)	Ground type (Short or Long)
AvgRoomB	OH, <0.01	Backyard, <0.05	>0.2
180HzAvgB	OH, <0.05	Backyard, <0.01	>0.2
AvgPerim	>0.2	Backyard, <0.01	>0.2
AvgChildB	OH, <0.01	Backyard, <0.01	>0.2
10%ChildB	OH, <0.01	Backyard, <0.01	Long, <0.05
AvgGC	OH, <0.01	>0.2	Short, =0.01
10%GC	OH, <0.01	>0.2	Short, <0.01
AvgV$_{OC}$	<0.2	Backyard, <0.001	Long, <0.001
10%V$_{OC}$	<0.2	Backyard, <0.001	Long, <0.001

Table shows *P*-value associated with regression coefficients of predictor variable; $P < 0.2$ means $0.10 < P < 0.2$; $P < 0.1$ means $0.05 < P < 0.1$; $P < 0.05$ means $0.01 < P < 0.05$; $P < 0.01$ means $0.001 < P < 0.01$. In one case $P = 0.01$.

Table also shows which predictor causes exposure to rise for all cases when $P<0.05$, e.g., AvgGC increases with Short Ground Type, compared to Long, and AvgRoomB increases with OH Line Type, compared to UG.

TABLE 5. Pearson Correlation of Average Exposure Parameters ($N=40$)

	180HzAvgB	AvgPerimB	AvgChildB	AvgGC	AvgV$_{OC}$
AvgRoomB	0.99	0.84	0.78	0.54	0.68
180HzAvgB	—	0.84	0.80	0.50	0.73
AvgPerimB		—	0.74	0.47	0.66
AvgChildB			—	0.65	0.93
AvgGC				—	0.37

The Ground Type main term (the α_2 term) contributes negligibly to explaining AvgV$_{OC}$ or AvgChildB. In other words, within each Location stratum (Backyard or Street) both AvgV$_{OC}$ and AvgChildB in our model are determined solely by ground current plus ground current as modified by the length of the ground path. For AvgRoomB, the same model explains 45% of the variance for Backyard and 72% of the variance for Street; for AvgPerimB, the model explains 47% of the variance for Backyard and 46% of the variance for Street. For neither AvgRoomB nor AvgPerimB were the main Ground Type or interaction terms statistically significant. Thus, across the full population of our model neighborhood, V$_{OC}$ and the child's magnetic field exposure classify each other better than any of the other field or ground current quantities.

Comparative Dosimetry

Finally, we compare dosimetric quantities averaged within the bone marrow and across the heart of an adult male resulting from magnetic field exposure, electric field exposure, and contact current, all 60 Hz. Although an important focus of these comparisons concern children, more precise modeling data are available for adults than for children. For this comparison, a uniform magnetic field of 10 µT, oriented perpendicular to the front of the body was chosen; the electric field chosen was 100 V/m, vertical and uniform when unperturbed; two electric field results are presented, one for a grounded subject and one for a subject in free space (off ground). These values represent extremely high residential fields that do not occur away from appliances. Contact current was estimated from the upper 10% average V$_{OC}$ value of 90 mV (see Table 2). Assuming a total body resistance (R_P) of 2.5 kΩ (see Reilly, 1998) and the same value back to the circuit ground (R_G), for a total resistance of 5 kΩ, we calculated a contact current of 18 µA, more than ten times below the median perception threshold for adult males (0.36 mA) [IEEE, 1985]; based on limited data for children in IEEE [1985], we estimated that the perception threshold for a child would be about 35–50% of the value listed for adult males (on the order of 0.15 mA). Of course, for hand-to-feet contact, current would double in a very well-grounded person, but would be much less, or even zero, for an individual wearing well-insulated footwear or standing on an insulated floor surface.

P. 39

TABLE 6. Comparative Dosimetry from Magnetic Field, Electric Field, and Contact Current Exposure[a]

Factor	Configuration	60 Hz exposure	Bone marrow		Heart		Reference
			E (mV/m)	J (mA/m^2)	E (mV/m)	J (mA/m^2)	
Magnetic field	Uniform, horizontal, perpendicular to front of body	10 µT	1.6×10^{-1}	8.0×10^{-3}	1.4×10^{-1}	1.4×10^{-2}	Dawson and Stuchly, 1998
Electric field	Uniform, vertical, grounded model	100 V/m	3.2×10^{-1}	1.6×10^{-2}	1.3×10^{-1}	1.3×10^{-2}	Stuchly et al., 1998
Electric field	Uniform, vertical, free space model	100 V/m	1.0×10^{-1}	5.0×10^{-3}	6.6×10^{-2}	6.6×10^{-3}	Stuchly et al., 1998
Contact current	Current injection into shoulders	18 µA (total)	3.5×10^{0}	1.8×10^{-1}	1.9×10^{0}	1.9×10^{-1}	Dawson et al., in press[b]

[a]The electric fields and current density values are averaged across the tissue.
[b]This reference reports dosimetry relevant to pacemaker interference only; tissue average values for this table provided by M. Stuchly (personal communication).
σ(heart) = 0.1 S/m
σ(marrow) = 0.05 S/m

The induced average electric fields and current densities (Table 6) were derived from values published by Stuchly and colleagues (references listed in table). These investigators used the scalar potential finite difference and finite-difference time-domain methods to calculate induced electric fields and current densities from fields and injected currents in anatomically correct models of adult males subdivided into cuboidal voxels 3.6 mm on a side, with tissue-specific conductivity, as estimated from published sources.

Table 6 reports that 18 µA injected current produces an electric field of 3.5 mV/m averaged across bone marrow and 1.9 mV/m averaged across heart tissue, more than an order of magnitude higher than from the field levels selected for comparison.

DISCUSSION

Our initial objective was to explore a possible engineering basis for the result of Ebi et al. (1999) that, in two previous studies of power lines and childhood cancer [Savitz et al., 1988; London et al., 1991], risk was related to the backyard location of lines, in contrast to street location. To that end, we developed a virtual neighborhood of 40 single-dwelling houses with different combinations of residential electric service attributes, including line location, line type, and ground length, as described above in detail. We report higher power-frequency and harmonic fields associated with overhead lines located in the backyard, higher ground currents associated with overhead lines and short ground paths, and higher open circuit voltage (V_{OC}) associated with backyard lines and long ground paths. Further, we find (a) V_{OC} is highly correlated with the magnetic field across the residential floor area (AvgChildB) in the neighborhood model; and (b)

compared to magnetic or electric fields, V_{OC} can produce a higher electric field in target tissue. As further discussed below, these last two results suggest that V_{OC} is a potentially relevant, though overlooked, exposure in prior studies concerned with the relationship of electric power line environments to health.

Correlation of Magnetic Fields With V_{OC}

The correlation of magnetic fields with V_{OC} in our virtual neighborhood reflects their fundamental electrical relationship. Both result from electrical current, the former from any current source near or in a residence and the latter from current in the ground. The high correlation of V_{OC} with AvgChildB for the neighborhood indicates that, in locations with similar electrical characteristics, the magnetic field measured across a residential area would serve as a marker or surrogate for V_{OC}. In actual neighborhoods, a poorer correlation is likely to occur. For example, currents on primary distribution lines that do not contribute to a given residence's ground current will nonetheless contribute to the residential field. Likewise, the correlations reported here do not extend to magnetic fields calculated for residences near overhead transmission lines based on historical load data, as was done for several Scandinavian epidemiology studies [reviewed in NIEHS Working Group, 1998]. Without further investigation, however, we would not categorically dismiss the possibility of contact potentials resulting from magnetic induction on long conductive paths within and between residences abutting rights-of-way.

We designed the neighborhood according to the "multi-ground neutral" practice required in the US, in which the chassis wire, the ground wire, and the utility neutral are electrically connected with each other at the

service panel. As a consequence, current in the ground will create a voltage source of magnitude V_{OC} at the chassis, which can drive a small "leakage" or contact current into an individual who contacts it (Figure 2). Several European countries, have used grounding practices that keep the chassis wire separate from the ground return pathway, leaving a much lower possibility for contact current [Rauch et al., 1992].

It is important to observe that V_{OC} is a characteristic of the residence itself, as determined by its electrical supply and grounding characteristics. Thus, all plugged-in devices with a conductive exterior surface will carry an equivalent V_{OC}, regardless of location in the residence. In contrast, high magnetic fields are often confined to "hot spots" associated with service drops, ground return pathways, or unusual wiring. Such hot spots may be away from areas that are normally occupied.

Dosimetry

As shown in Table 6, contact currents far below perception thresholds produce electric fields in tissue that exceed those due to ambient residential magnetic fields (away from appliances). We compared a contact current due to time-averaged V_{OC} within the upper tail of this parameter's distribution across the neighborhood to a uniform magnetic field ($10 \mu T$) larger by a factor of at least 10–20 than the highest space and/or time-averaged residential magnetic fields measured in many US studies [reviewed in Kavet, 1995]. Near appliances the fields may be even higher than $10 \mu T$, but they are highly nonuniform in space falling off usually with the cube of distance from the device.

The dosimetric contrasts shown in Table 6 for adults would likely be accentuated for child-size subjects. As Kaune et al. [1997] have shown in analytical solutions of simple ellipsoidal models, induced electric fields and current densities from the same electric and magnetic fields as above would be lower due to reduced coupling to the smaller body size. With the dimensions Kaune et al. [1997] used, coupling in children was about 30% lower for both magnetic and electric fields. For contact potentials, although total body impedance is higher for children (approximately 40–50%, see Reilly [1998]), their reduced cross sectional area (roughly half or less of an adult) results in larger induced quantities. Further, the marrow dose for contact current shown in Table 6 was based on bilateral current injection into the shoulders [to analyze pacemaker interference (Dawson et al., in press)]. The tissue levels shown in the table are averaged across the body even though, for shoulder injection, the current through the arm is negligible.

Thus, for hand-to-feet conduction, the current would pass through the long bones of a single arm, which has a smaller cross section than the leg, the net effect of which would be higher induced quantities in the exposed upper extremity.

In addition to these relative aspects of dose, the absolute (as well as modest) level of contact current modeled ($18 \mu A$) produces average electric fields in tissue along its path that exceed $1 mV/m$. At and above this level, the NIEHS Working Group [1998] accepts that biological effects relevant to cancer have been reported in "numerous well-programmed studies". The effects the Working Group cites are "increased cell proliferation, disruption of signal transduction pathways, and inhibition of differentiation". The NIEHS endorses this conclusion in its final EMF RAPID report [1999].

Nonetheless, it remains important to compare electric fields induced in tissue due to environmental exposure to the magnitude and spectra of fields due to endogenous electrical activity. Hart and Gandhi [1998] report that the average 40–70 Hz endogenous electric field in cardiac tissue is between 8 and 25 mV/m, depending on computational method. The cardiac signal decreases with distance to neighboring tissue and is negligible in the brain. Natural electrical activity in the central nervous system (CNS), as recorded on the electroencephalogram, may be several millivolts per meter (see NIEHS, 1997), peaks below 30 Hz and has little spectral power beyond 40 Hz.

Bone marrow, target tissue for leukemia, is located directly adjacent to bone tissue, which when physically loaded, experiences "streaming potentials" of up to $0.1–1 V/m$ [MacGinitie, 1995; reviewed in NIEHS Working Group, 1998]. In general, the spectral power of these potentials is mainly below 10 Hz [McLeod et al., 1998]. The extent to which these fields extend to the marrow is not known precisely, although they tend to be radially oriented and would not be expected to produce marrow fields that exceed $1 mV/m$. Although cartilage has streaming potentials even higher than bone, the physical and electrical relations of cartilage to bone marrow are also likely to result in only small fields in the marrow [K. McLeod, personal communication]. Finally, active skeletal muscle produces local extremely-low-frequency (ELF) electric fields due to ongoing action potential activity. However, given the relative resistance of muscle and bone, the resulting fields normal to the bone are expected to remain confined to the muscle layer itself with little effect inside the marrow; some penetration of the component parallel to bone will occur due to boundary effects, but is likely to be attenuated in the marrow. Thus, the marrow of the long

P. 41

bones, site of hematopoiesis and leukemogenesis in humans, is most likely electrically silent with respect to natural ELF signals in the heart and CNS (due to distance), and based on first principles, quite likely "quiet" due to bone and muscle activity nearby. However, further microdosimetric research will be required to clarify the natural electric field environment inside bone marrow.

Epidemiological Implications

In a pooled analysis of all "qualifying" worldwide studies concerned with residential magnetic fields and childhood leukemia published through 1998, Greenland et al. (submitted) report a summary relative risk of 1.8 (95% CI: 1.1–2.9) associated with fields greater than $0.3 \, \mu T$, compared to $< 0.1 \, \mu T$, with no evidence of heterogeneity across studies or across continents. In contrast, the risks associated with high wire categories (relevant to US studies only) were not consistent across studies.

Since the pooled analysis was completed, two studies of leukemia among children in Canada have been published, with neither reporting excess risk associated with wire code. McBride et al. [1999] reported little indication of an association of leukemia with personally monitored fields, while Green et al. [1999a] showed elevated odds ratios associated with fields measured within the residence and around the residence perimeter, as well as with the exposures recorded on personally-worn monitors [Green et al., 1999b]; these elevated risks were concentrated among younger children. A study across England, Wales, and Scotland [UKCCSI, 1999] reported no excess risks of childhood leukemia (or other cancers) associated with measured residential magnetic fields. How these more recent results may affect the pooled analysis has not been determined.

The immediate application of our results to specific studies in the EMF childhood leukemia literature is limited. The neighborhood was configured to represent residential electric service scenarios found in the Denver [Savitz et al., 1988] and Los Angeles [London et al., 1991] studies to address findings unique to those data sets [Ebi et al., 1999].

To that end, the neighborhood model incorporated realistic housing dimensions and realistic distances from the residence to street facilities (utility line and water main) and to backyard lines. The loads on the service drop conductors and 3rd harmonic generated from residential electricity usage were based on data acquired in a large-scale survey of nearly 1000 homes in the US [Zaffanella, 1993]. The power lines serving the neighborhood, however, were not loaded in accordance with their current-carrying capacity, nor

were transformers more heavily concentrated on three-phase primaries, as compared to the other primaries in the model. Accordingly, the model neighborhood's power delivery system analyzed in this paper did not (and was not intended to) simulate the Wertheimer-Leeper wiring configurations, as they have been used in many epidemiological and exposure assessment studies.

In our simulated neighborhood, in which overhead distribution currents played no role in producing residential fields, the Spearman correlation of AvgGC with RoomAvgB was 0.52; in a sample of 333 nationwide residences whose magnetic fields were minimally affected by overhead power lines [see Kavet et al., 1999], the Spearman correlation of 24 h average ground current with spot measurements averaged across the residence was 0.41 [Kavet, unpublished observation]. Whereas the latter correlation was with respect to a field measurement taken at one point of time during the day in the real world, compared to a time averaged room measurement computed in a simulated neighborhood, the correspondence of these two correlation values is reassuring with regard to the neighborhood's representativeness of service drop/ground electrical properties.

V_{OC} is an exposure variable that we believe could explain the marginal association of measured field with leukemia in the Denver study (odds ratio (OR) of 1.93, 95% confidence interval (CI) 0.67–5.56; $\geq 0.2 \, \mu T$ spot-measured field compared to $< 0.2 \, \mu T$), and in the Los Angeles study (OR of 1.48, 95% CI 0.66–3.29; $\geq 0.268 \, \mu T$ 24 h bedroom average compared to $< 0.68 \, \mu T$). Both of these studies also reported positive associations between Wertheimer-Leeper wire code and leukemia risk, as well as positive associations between wire code and measured fields. As Ebi et al. [1999] reported, the wire code/leukemia associations in both studies were confined to backyard lines. Here, we report that both magnetic fields and V_{OC} are higher in residences with backyard lines.

In a separate follow-up analysis of the Savitz et al. (1988) Denver data set, Wertheimer et al. [1995] reported that increased all-cancer risks were associated with conductive plumbing, as well as with a metric they termed "elevated non-vertical" (ENV) fields, a marker of magnetic fields due to ground currents. These ENV fields may well have served as markers for V_{OC} according to the engineering relationships presented in this paper. No similar data were explicitly reanalyzed for Los Angeles, although Bowman et al. [1999] created a predictive model for residential magnetic fields in that data set which was used to confirm an association of leukemia risk with magnetic fields [Thomas et al., 1999]. These investigators

conclude that the predicted fields cannot entirely account for the wire code association with leukemia reported by London et al. [1991], and that "the most likely hypothesis is that an unidentified exposure metric involving the ELF magnetic field plays a role in carcinogenesis". Although the investigators are likely alluding to alternate field metrics (perhaps transients), we believe that in a broader context, a "metric involving the ELF magnetic field" could also include contact current.

In the nine-state National Cancer Institute (NCI) childhood leukemia study [Linet et al., 1997], excess risk was reported for fields above $0.3\,\mu T$ "blended" time-average field relative to $<0.065\,\mu T$ (OR 1.7; 95% CI 1.0–2.9); in the $0.4–0.5\,\mu T$ stratum, the OR peaked at 3.3 (95% CI 1.2–9.4). At higher fields the OR fell. We can only conjecture that the absence of a monotonic risk function in this study is due to the fact that the highest fields in the NCI data are caused by sources, such as nearby high voltage transmission lines, which do not contribute current to the residential ground path and thus to V_{OC}, whereas risk peaked among residences with high fields created by ground currents with correlated increases in V_{OC}. The NCI study reported no relationship of leukemia risk with Wertheimer-Leeper wire code category.

As mentioned above, the model here does not in any obvious way, adequately explain positive associations of cancer with overhead high voltage transmission lines, as reported in Sweden by Feychting et al. [1993]. However, we note the absence of a positive association in the study of childhood leukemia across the United Kingdom [UKCCSI, 1999], where residential wiring practices may preclude contact currents of the magnitude prevalent in residential electrical systems in the US.

Limitations

At this time there are no data that describe (a) the distribution of V_{OC} across residences, both single dwelling and multioccupancy, (b) the extent of physical contact with energized equipment or other conductive objects in the home that could produce contact current, or (c) the currents that actually result from such contacts. Factors that affect the magnitude of current from such contact include a residence's service/ground configuration and time-varying net load, alternative current paths (hand-to-hand and hand-to-feet), and variable impedance back to ground.

In addition, other situations can lead to either high V_{OC} or V_{OC} on unintended surfaces. For example, a poor connection in the service drop neutral will increase current through the ground wire, which will increase V_{OC}. Although all water pipes were assumed

at ground in the model, a poorly conductive joint in a water line can produce V_{OC} on water fixtures if the ground wire is bonded upstream of that joint.

We need to address the data gaps identified above from a historical, as well as contemporary, perspective. Historical, to understand previous epidemiology studies of cases that occurred up to decades ago, when appliance construction, home wiring practices, and water service were different than they are today. More appliances today have a plastic exterior compared to metal exterior surfaces prevalent years ago; three-hole and two-hole polarized sockets are standard today as opposed to the unpolarized two-wire sockets used previously; and water service has evolved from copper pipe to plastic pipe, resulting in more alternative grounding practices. Contemporary, because if V_{OC} is an important exposure parameter with respect to health risks, then the knowledge of exposure characteristics as they now occur is critical to the design of new epidemiology studies. Obtaining reasonable estimates of the magnitude and temporal quality (likely to be highly intermittent) of residential contact current exposures, both historically and contemporarily, will also assist in designing laboratory studies to determine if appropriate cell or animal models of leukemia respond to exposures representative of the real world.

Another factor concerns exposures in apartment buildings, in which individual units are served through separate electric meters served from the same service drop. About one-quarter of all housing units in the US are apartments [US Census Bureau, 1999]. Depending on the wiring in the building, V_{OC} in one apartment may be dependent, to some extent, on net loads serving the others.

Other potentially relevant aspects of residential distribution systems have not been addressed here. These would include possible effects from loads downstream of the neighborhood in terms of fields from the primaries associated with those loads, and ground return currents that can insinuate themselves into the neighborhood's grounding system. All of the grounding in the neighborhood was through conductive water pipe through a conductive water main. The analysis here did not address redistribution of return current due to alternate grounding methods, such as driven ground rods or the effect of unintentional faults in the grounding system.

CONCLUSION

We have identified contact current due to V_{OC} as a factor potentially responsible for the association between residential magnetic fields and childhood leukemia. The studies of childhood leukemia risks in

EMF environments, which were of case-control design, encompass diverse combinations of base populations, control selection methods, transmission and distribution systems, and methods for assessing historical exposure relevant to a proposed etiologic period. Although alternate environmental exposures, including local vehicular traffic density [Pearson et al., 1999], viral contact [Sahl, 1994], and water quality [Kavet, 1995] have been proposed as possible explanations, none have risen to an acceptable level of plausibility. In addition, no bias with respect to case-control selection or response has been identified that would rationalize the positive associations in any unifying way [NIEHS Working Group, 1998]. The NIEHS Working Group's report [1998] and the NIEHS EMF RAPID report [1999] both concluded that significant uncertainty remains with respect to childhood leukemia risk in magnetic field environments.

In the virtual neighborhood analyzed here, which models residential service for single dwelling homes across much of the US and Canada, V_{OC} is strongly associated with the magnetic field, and is capable of delivering biologically significant dose to target tissue. Our conclusion regarding V_{OC} is more difficult to rationalize for those studies reporting positive associations in an overhead transmission line environment, although exposed caseloads were extremely small in number and magnetic induction effects cannot be ruled out automatically. The pooled analysis by Greenland et al. (submitted) suggests increased childhood leukemia risk above $0.3\,\mu T$, indicative of large currents in and around the residence. In our model, large currents in the ground are also capable of generating high V_{OC}. Interestingly, there has been no trace of positive association of childhood leukemia with residential electric fields [Savitz et al, 1988; London et al., 1991; McBride et al., 1999], which may be present regardless of current flow.

Two-year bioassays, as well as shorter-term model-specific bioassays for magnetic field carcinogenicity, and leukemia in particular, have been almost entirely negative [McCann et al., 1997, 2000] and have created a conceptual obstacle for drawing inferences regarding magnetic fields as a possible leukemogen [NIEHS, 1999]. If a toxicologically significant dose (induced electric field) is required in the fore- and hindlimbs to promote leukemia in a rodent model, then a magnetic field, even the high fields used in the bioassays, may be ineffective because of poor coupling to those sites.

To date there is no accepted biophysical mechanism that would explain leukemogenic effects of residential-strength magnetic fields, which are $<1\,\mu T$ away from appliances [Valberg et al., 1997; NIEHS

Working Group, 1998]. Contact currents due to V_{OCS} of the magnitude estimated for the residences in our neighborhood model produce electric fields in tissue that do not strain the question of biological plausibility to this extent, and in fact, produce doses with the potential to trigger biological effects.

Many unknowns about contact currents resulting from V_{OC} remain with respect to biological effects in appropriate laboratory models, the extent of exposure across the population now and historically, and the relevant associations of exposure with health endpoints. Finally, contact current is an exposure that likely occurs in the workplace in association with energized equipment. Occupational exposures to contact current merit as much attention as do residential exposures.

ACKNOWLEDGMENT

APPENDIX 1

Detailed Neighborhood Description

1. Four streets and 40 houses comprise the model (Figure 3). A Street, B Street, and C Street run West to East, and N Street runs South to North. A Street and C Street are cul-de-sac, with 12 houses in A Street and six in C Street included in the study. B Street and N Street are through streets. Twelve houses in B Street and 10 in N Street are included in the study. A Street, B Street, and C Street are 12.2 m (40 feet) wide. N Street is 19.8 m (65 feet) wide. Houses are set back 9.1 m (30 feet) from the street.

2. A three-phase overhead distribution line, with thick wires (the term, "thick", was used by Wertheimer and Leeper [1979] to describe lines with high potential loading), is running along N Street. Another three-phase overhead distribution line, with thick wires, is running in the backyards of houses between A and B Streets. An overhead distribution line with a single-phase primary is running in the backyards of houses between B and C Streets. An underground distribution line serves the houses on the North side of A Street. The height of the neutral above ground is 10.1 m (33 feet). The distances between houses and lines are shown in Figure 3 and are listed in Appendix 2.

3. Seven different distribution transformers (T1 to T7) serve different groups of houses as shown in Figure 3. The transformers are connected between one phase of the primary and the neutral. For instance, transformer T6 is connected between Phase C and the neutral and serves eight houses: four houses directly connected to the transformer and four houses connected at the end of a secondary line.

4. The segments of the ground current circuit are indicated with thicker lines. They include water mains, water service lines connecting houses to the main, and the conductors connecting the electrical service neutral to the water service line inside the houses ("grounding wires"). The water mains are located in the middle of the street, 1.1 m (3.6 feet) below street level. Two types of ground current paths are considered inside each house: type 1 and type 2 (Figure 4). Type 1 is the shorter possible path for overhead street lines, overhead backyard lines, and underground street lines (top to bottom in Figure 4). Type 2 is the longer possible path for overhead street lines, overhead backyard lines, and underground street lines (top to bottom in Figure 4). For each house, the service drop arrives at a corner and then goes to the electrical panel. The attachment points of overhead service drops at the houses are 5.3 m (17.4 feet) above street level. The distance between service drop and inside wall of the house is 0.5 m (20 inches). The grounding wire is 0.3 m (10 inches) below the first floor. The water service line from the main is perpendicular to the street and arrives at 0.3 m (1 foot) from a house

corner at a depth of 1.1 m (3.6 feet) below street level.

5. The class (1 = thick 3-phase primary, 3 = first span secondary, 6 = end pole, 7 = underground), distance, and wire code of the residences, the type of line (street or backyard), and the type of ground current path (Type 1 or Type 2) are listed in Appendix 2. Using Wertheimer-Leeper wire code terminology, there are 11 Very High Current Configuration (VHCC) houses, 13 Ordinary High Current Configuration (OHCC) houses, two Ordinary Low Current Configuration (OLCC) houses, and 14 Very Low Current Configuration (VLCC) houses, six of which have underground service.

6. The same dimensions are assigned to all houses: two-floor houses with a rectangular floor plan 10.7 m by 7.6 m (35 × 25 ft), with the longest dimension parallel to the street. The first and second floors are at 0.5 m (1.6 feet) and 3.3 m (10.8 feet) above street level, respectively. Each house contains eight equal size rooms, four per floor.

7. The electrical parameters of the conductors of the ground current circuit are given in Appendix 3. The values of these parameters were chosen to represent values encountered in practical situations. The termination impedances (to ground) simulating the extension of water mains and primary neutrals beyond the immediate neighborhood are listed in Appendix 3. The primary loads and their return currents had a negligible effect on residential magnetic fields and ground currents, and, therefore, were not taken into account in the neighborhood analysis presented in the Results.

APPENDIX 2

Characteristics of Neighborhood Houses

House	Class	Distance m (feet)	Residence code	Line type	Line location	Ground type
A1	7	7.6 (25)	VLCC	UG	Street	1
A2	1	13.7 (45)	VHCC	3-Phase	Backyard	1
A3	7	7.6 (25)	VLCC	UG	Street	2
A4	1	13.7 (45)	VHCC	3-Phase	Backyard	2
A5	7	7.6 (25)	VLCC	UG	Street	2
A6	1	13.7 (45)	VHCC	3-Phase	Backyard	1
A7	7	7.6 (25)	VLCC	UG	Street	1
A8	1	13.7 (45)	VHCC	3-Phase	Backyard	2
A9	7	7.6 (25)	VLCC	UG	Street	1
A10	1	13.7 (45)	VHCC	3-Phase	Backyard	2
A11	7	7.6 (25)	VLCC	UG	Street	1
A12	1	13.7 (45)	VHCC	3-Phase	Backyard	1
B1	1	24.4 (80)	OHCC	3-Phase	Backyard	2
B2	6	13.7 (45)	VLCC	1-Phase	Backyard	2
B3	1	24.4 (80)	OHCC	3-Phase	Backyard	2
B4	3	13.7 (45)	OHCC	1-Phase	Backyard	1
B5	1	24.4 (80)	OHCC	3-Phase	Backyard	1
B6	3	13.7 (45)	OHCC	1-Phase	Backyard	1

P.'45

House	Class	Distance m (feet)	Residence code	Line type	Line location	Ground type
B7	1	24.4 (80)	OHCC	3-Phase	Backyard	1
B8	6	13.7 (45)	VLCC	1-Phase	Backyard	2
B9	1	24.4 (80)	OHCC	3-Phase	Backyard	1
B10	6	13.7 (45)	VLCC	1-Phase	Backyard	2
B11	1	24.4 (80)	OHCC	3-Phase	Backyard	2
B12	6	13.7 (45)	VLCC	2-Phase	Backyard	1
C1	6	24.4 (80)	VLCC	2-Phase	Backyard	1
C3	3	24.4 (80)	OLCC	2-Phase	Backyard	2
C5	3	24.4 (80)	OLCC	2-Phase	Backyard	1
C7	6	24.4 (80)	VLCC	2-Phase	Backyard	2
C9	6	24.4 (80)	VLCC	2-Phase	Backyard	2
C11	6	24.4 (80)	VLCC	2-Phase	Backyard	1
N1	1	13.7 (45)	VHCC	3-Phase	Street	1
N2	1	24.4 (80)	OHCC	3-Phase	Street	1
N3	1	13.7 (45)	VHCC	3-Phase	Street	1
N4	1	24.4 (80)	OHCC	3-Phase	Street	1
N5	1	13.7 (45)	VHCC	3-Phase	Street	2
N6	1	24.4 (80)	OHCC	3-Phase	Street	1
N7	1	13.7 (45)	VHCC	3-Phase	Street	1
N8	1	24.4 (80)	OHCC	3-Phase	Street	2
N9	1	13.7 (45)	VHCC	3-Phase	Street	2
N10	1	24.4 (80)	OHCC	3-Phase	Street	2

APPENDIX 3

Electrical Parameters of the Ground Current Circuit Conductors[a]

	Resistance (mΩ/m)	Geometric mean diameter (m)
Primary neutral	0.494	0.008
Secondary neutral (overhead line)	0.494	0.008
Secondary neutral (underground line)	0.336	0.009
Service drop neutral (overhead)	0.494	0.008
Service drop neutral (underground)	0.84	0.005
Grounding wire	3.25	0.0025
Water line	0.206	0.023
Water main[b]	0.32	0.01
Ground rod at service entrance	50 Ω	
Water main terminations	0.002 Ω	
Primary neutral terminations	0.002 Ω	

[a]The values in the table are based on personal experience of one of the authors (LEZ), who managed the EPRI high voltage facility in Lenox, MA, was the principal investigator of the "1000-home study" [Zaffanella, 1993], and developed the algorithms for the ground current network analysis used in the modeling software.
[b]Geometric mean diameter (GMD) is a function of a conductor's physical dimensions and impedance characteristics. The water main has a smaller GMD than the water line, even though it is physically larger.

REFERENCES

Barnes F, Wachtel H, Savitz D, Fuller J. 1989. Use of wiring configuration and wiring codes for estimating externally generated electric and magnetic fields. Bioelectromagnetics 10:13–21.

Bowman JD, Thomas DC, Jiang L, Jiang F, Peters JM. 1999. Residential magnetic fields predicted from wiring configurations: I. Exposure model. Bioelectromagnetics 20: 399–413.

Dawson TW, Stuchly MA, Caputa K, Sastre A, Shepard RB, Kavet R. Pacemaker interference and low frequency electric induction in humans by external fields and electrodes. IEEE Trans Biomed Eng. (In press).

Dawson TW, Stuchly MA. 1998. High-resolution organ dosimetry for human exposure to low-frequency magnetic fields. IEEE Trans Magnetics 34:708–718.

Ebi KL, Zaffanella LE, Greenland S. 1999. Application of the case-specular method to two studies of wire codes and childhood cancers. Epidemiology 10:398–404.

Feychting M, Ahlbom A. 1993. Magnetic fields and cancer in children residing near Swedish high-voltage power lines. Am J Epidemiol 138:467–481.

Green L, Miller A, Agnew D, Greenberg M, Li J, Villeneuve P, Tibshirani R. 1999a. Childhood leukemia and personal monitoring of residential exposures to electric and magnetic fields in Ontario, Canada. Cancer Causes Control 10: 233–243.

Green L, Miller A, Villeneuve P, Agnew D, Greenberg M, Li J, Donnelly K. 1999b. A case-control study of childhood leukemia in southern Ontario, Canada, and exposure to magnetic fields in residences. Int J Cancer 82:161–170.

Greenland S, Shepard A, Kelsh M, Kaune W. A pooled analysis of magnetic fields, wire codes and childhood leukemia. (submitted).

Hart RA, Gandhi OP. 1998. Comparison of cardiac-induced endogenous fields and power frequency induced exogenous fields in an anatomical model of the human body. Phys Med Biol 43:3083–3099.

IEEE. 1985. Corona and field effects of AC overhead transmission line: information for decision makers. IEEE Power Engineering Society, New York, NY.

International Commission on Non-Ionizing Radiation Protection. 1998. Guidelines for limiting exposure to time-varying electric, magnetic, and electromagnetic fields (up to 300 GHz). Health Physics 74:494–522.

Kaune WT, Guttman JL, Kavet R. 1997. Comparison of coupling of humans to electric and magnetic fields with frequencies between 100 Hz and 100 kHz. Bioelectromagnetics 18:67–76.

Kavet R. 1995. Magnetic field exposure assessment. In: Blank M, editor. Electromagnetic fields: biological interactions and mechanisms. Washington, DC: American Chemical Society, p 191–223.

Kavet R, Ulrich R, Kaune W, Johnson G, Powers T. 1999. Determinants of power-frequency magnetic fields in residences located away from overhead power lines. Bioelectromagnetics 20:306–318.

Kheifets LI, Kavet R, Sussman SS. 1997. Wire codes, magnetic fields, and childhood cancer. Bioelectromagnetics 18:99–110.

Linet MS, Hatch EE, Kleinerman RA, Robison LL, Kaune WT, Friedman DR, Severson RK, Haines CM, Hartsock CT, Niwa S, Wacholder S, Tarone RE. 1997. Residential exposure to magnetic fields and acute lymphoblastic leukemia in children. N Engl J Med 337:1–7.

London SJ, Thomas DC, Bowman JD, Sobel E, Cheng T-C, Peters JM. 1991. Exposure to residential electric and magnetic fields and risk of childhood leukemia. Am J Epidemiol 134:923–937.

MacGinitie LA. 1995. Streaming and piezoelectric potentials in connective tissue. In: Blank M, editor. Electromagnetic fields: biological interactions and mechanisms. Wash, DC: American Chemical Society, p 125–142.

McBride M, Gallagher R, Theriault G, Armstrong B, Tamaro S, Spinelli J, Deadman J, Fincham S, Robson D, Choi W. 1999. Power-frequency electric and magnetic fields and risk of childhood leukemia in Canada. Am J Epidemiol 149:831–842.

McCann J, Kavet R, Rafferty CN. 1997. Testing EMF for potential carcinogenic activity: a critical review of animal models. Environ Health Perspect 105 (Suppl 1):81–103.

McCann J, Kavet R, Rafferty CN. 2000. Assessing the potential carcinogenic activity of magnetic fields using animal models. Environ Health Perspect. 108 (Suppl 1): 79–100.

NEC. 1992. National Electric Code 1993. Quincy, MA: National Fire Protection Association.

McLeod KJ, Rubin CT, Otter MW, Qin Y-X. 1998. Skeletal cell stresses and bone adaptation. Am J Med Sci 316:176–183.

NESC. 1992. 1993 National Electric Safety Code. New York, NY: IEEE.

NIEHS. 1997. EMF Science Review Symposium: Breakout Group Reports for theoretical mechanisms and in vitro research findings. March 24–27, 1997. National Institutes of Environmental Health Sciences, Durham, NC.

NIEHS Working Group. 1998. Assessment of health effects from exposure to power-line frequency electric and magnetic fields: working group report. Portier C, Wolfe M, editors. NIH Publication No. 98-3981. National Institute of Environmental Health Sciences. Research Triangle Park, NC.

NIEHS. 1999. Health effects from exposure to power-line frequency electric and magnetic fields. NIH Publication No. 99-4493, Research Triangle Park, NC.

Pearson RL, Wachtel H, Ebi KL. 1999. Traffic density as a risk factor for childhood cancer in Denver and Los Angeles. EPRI, TR-114231, Palo Alto, CA.

Rauch GB, Johnson G, Johnson P, Stamm A, Tomita S, Swanson J. 1992. A comparison of international residential grounding practices and associated magnetic fields. IEEE Trans Power Delivery 7:934–939.

Reilly JP. 1998. Applied bioelectricity: from electrical stimulation to electropathology. New York: Springer-Verlag.

Sahl JD. 1994. Viral contacts confound studies of childhood leukemia and high-voltage transmission lines. Cancer Causes Control 5:279–283.

Savitz DA, Wachtel H, Barnes FA, John EM, Tvrdik JG. 1988. Case-control study of childhood cancer and exposure to 60-Hz magnetic fields. Am J Epidemiol 128:21–38.

Stuchly MA, Dawson TW, Caputa K, Okoniewski M, Potter M. 1998. Validation of computational methods for evaluation of electric fields and currents induced in humans exposed to electric and magnetic fields. EPRI, Report TR-111768, Palo Alto, CA.

Thomas DC, Bowman JD, Jiang L, Jiang F, Peters JM. 1999. Residential magnetic fields predicted from wiring configurations: II. Relationships to childhood leukemia. Bioelectromagnetics 20:414–422.

UK Childhood Cancer Study Investigators. 1999. Exposure to power-frequency magnetic fields and the risk of childhood cancer. The Lancet 354:1925–1931.

US Census Bureau. 1999. Statistical Abstract of the United States, 1999. Washington, DC: US Census Bureau, 1999.

Valberg PA, Kavet R, Rafferty CN. 1997. Can low-level 50/60 Hz electric and magnetic fields cause biological effects? Radiat Res 148:2–21.

Wertheimer N, Leeper E. 1979. Electrical wiring configurations and childhood cancer. Am J Epidemiol 109:273–284.

Wertheimer N, Leeper E. 1982. Adult cancer related to electrical wires near the home. Int J Epidemiol 11:345–355.

Wertheimer N, Savitz DA, Leeper E. 1995. Childhood cancer in relation to indicators of magnetic fields from ground current sources. Bioelectromagnetics 16:86–96.

Zaffanella LE, Kavet R, Pappa JR, Sullivan TP. 1997. Modeling magnetic fields in residences: validation of the RESICALC program. J Exp Anal Environ Epidemiol 7:241–258.

Zaffanella LE. 1993. Survey of residential magnetic field sources. Electric Power Research Institute, TR-102759, Vol 1-2, Palo Alto, CA.

p. 47

EXHIBIT C

Electrical Stimulation and Electropathology
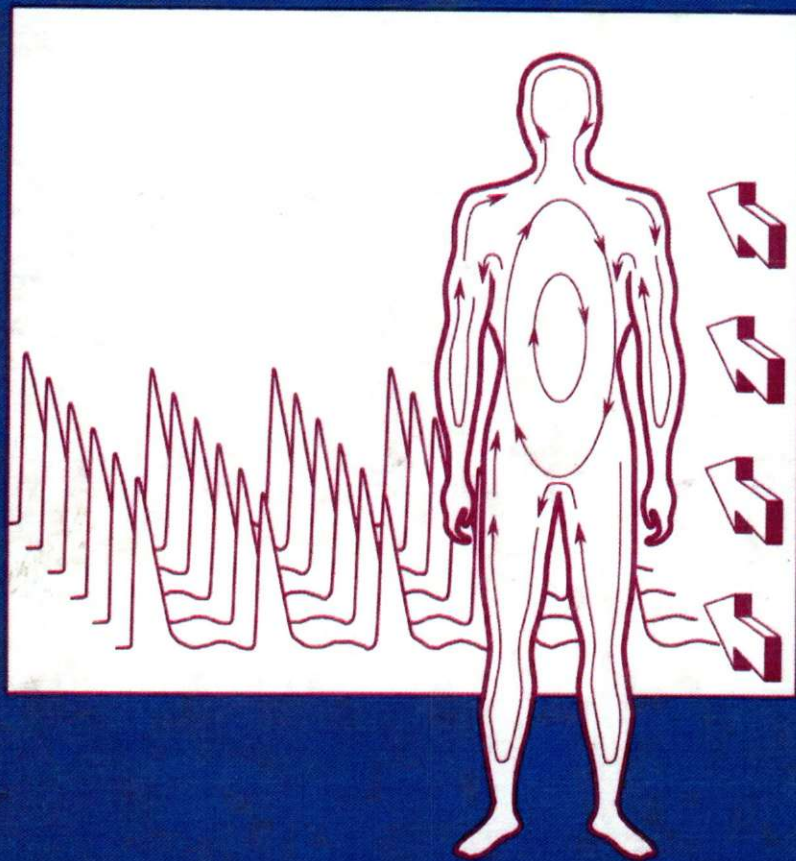
J. Patrick Reilly

Table 2.7. *Statistical summary of DC body impedance measurements (data listed in kΩ)*

	Adults			Children		
	5%	50%	95%	5%	50%	95%
A. Dry conditions						
Hand/hand	6.96	11.45	15.69	4.04	14.35	51.10
Hand/two feet	2.62	4.00	6.51	2.62	5.70	18.72
Hand/two feet	—	—	—	2.00	4.25	12.68
B. Wet conditions						
Hand/hand	1.28	1.86	2.45	1.70	2.55	4.47
Hand/two feet	0.93	1.20	1.67	1.43	1.80	3.02
Two hands/two feet	0.63	0.84	1.16	0.90	1.30	2.04

Notes: (a) Hand electrodes: two No. 10 Awg twisted copper wires.
(b) Voltage: 12 V DC; curent ~ 1 mA (children), ~ 5 mA (adults).
(c) Wet conditions apply to treatment with 20% NaCl solution.
(d) Children's ages: 3–15 years; adults ages: 18–58 years.
(e) Data from H. B. Whitaker (1939).

The curves plotted in Figs. 2.22 and 2.23 form approximately straight lines, which indicate the log-normal distribution on this plotting format. The slopes of the distribution curves are substantially less for wet than for dry conditions, and dry-skin slopes are greater for children than for adults. In general, children's resistance is greater than that of adults. Apparently, the shorter current paths of children is more than offset by their reduced volume. This can be appreciated by a simple calculation treating the limbs as conducting cylinders of length L and cross-sectional radius r. According to Eq. (2.1), the limb resistance would be calculated by $R = L\rho/(\pi r^2)$. If we assume that the ratio L/r is independent of body size, then it is concluded that resistance would vary inversely with r.

2.4   Impedance at Higher Frequencies

Skin impedance decreases as the frequency of the excitation current is increased, as noted in Table 2.8 (Schwan, 1968). The capacitive component of skin impedance is primarily responsible for its frequency dependence. Figure 2.24 illustrates the frequency dependence of impedance over the range 0–2000 Hz, using large hand-to-hand electrodes on dry skin (from Biegelmeier, 1986). At the highest frequency, impedance is reduced to about 750 Ω, a value approximately that for the internal body impedance with hand-to-hand contacts.

Figure 2.25 illustrates the measurements of Osypka (1963) in the frequency range 0.3–100 kHz, using low voltages (approximately 10 V) and

arge copper-cylinder hand-to-hand contacts. The test results with dry and wet hands show that above 5 kHz, the effects of skin hydration become negligible. Table 2.9 shows impedance measurements at 0.375 and 1 MHz (Schwan, 1968). The hand-to-hand data are similar to the values for internal body impedance as discussed in Sec. 2.3.

Chatterjee and colleagues (1986) measured impedance in the range of 10 kHz to 10 MHz. Adult subjects numbered 367 (170 M, 197 F). The hand electrode was a brass rod of diameter 1.5 cm; subjects stood barefoot on a copper plate. Prior to measurements, the subject's hand was moistened

Table 2.8. *Dry-skin impedance versus frequency*

Frequency (kHz)	Magnitude (Ω cm^2)	Phase angle (deg)
1	14,000	—
5	3,000	-70
10	1,800	-65
20	1,000	-55
50	500	-30
100	300	-20
200	250	-10

Note: Phase angle given by $\tan^{-1} X/R$, where X is capacitive reactance, and R is resistance.
Source: Schwan (1968).

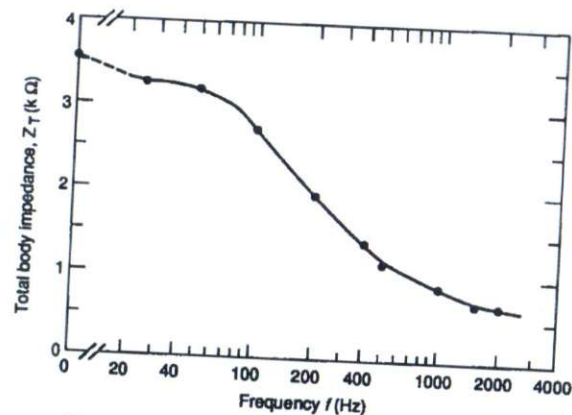Figure 2.24   Frequency dependence of impedance with large electrodes, dry hand-to-hand current path. Applied voltage = 25 V rms. (From Beigelmier, 1986.)

with 0.9% physiological saline. The subject's feet were not treated with saline. Figure 2.26 shows results from these experiments separately for male and female subjects. The authors assumed that impedance was related to body size, rather than sex per se, and that impedance was inversely proportional to subject's height. The phase-angle data show that the impedance is largely resistive in the indicated frequency range. The magnitude of impedance drops steadily with increasing frequency, to a

Table 2.9. *Body impedance at 0.375 and 1 MHz*

Electrode location	Area (cm^2)	Impedance $f = 0.375$ MHz (Ω)	$f = 1$ MHz (Ω)
Hand to hand	90	475	460
Finger to other arm	10/65	500	470
Across left arm	32	34	21
Across elbow joint	32	37	21
Across shoulder joint	32	47	31
Across neck	32	36	18
Forehead to neck	32	82	57
Chest to back	150	31	20
Across thorax	150	29	19
Right wrist to left leg	75	248	234
Left wrist to right leg	75	274	266

Note: Area applies to each electrode, except for finger/arm, where two different electrode sizes were used.
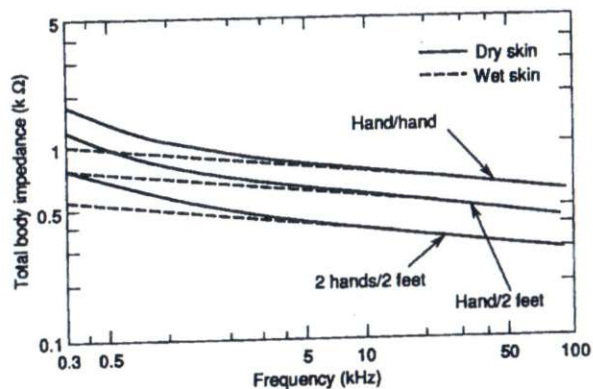*Source:* From Schwan (1968).

Figure 2.25   Total body impedance for large-area contacts in the frequency range 0.3–100 kHz. (From Osypka, 1963.)

value nearly equal to the internal body impedance reported in Sec. 2.3 for hand-to-feet contacts.

2.5   High-Voltage and Transient Properties

The author and colleagues studied current and voltage relationships under high-voltage conditions with living subjects (Reilly et al., 1983, 1984, 1985). These experiments could be safely conducted on living subjects because the duration and energy of the stimuli were limited by the use of capacitive discharges. These experiments provided the first detailed account of high-voltage current response in the microsecond time scale.
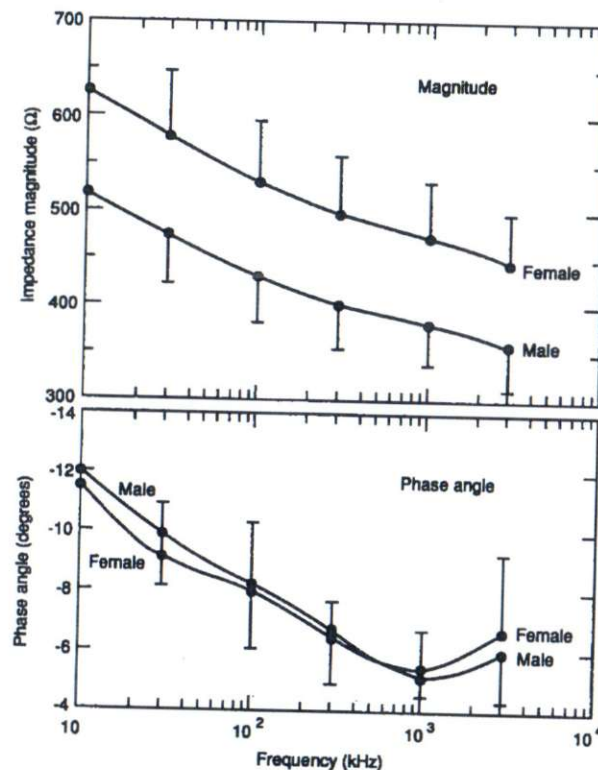

Figure 2.26   Magnitude and phase of impedance measured on 367 subjects, hand-to-feet contact. Hand electrode: 3.5-cm rod; wet hand contacts; bare feet on plate. Vertical bars show standard deviations. (From Chatterjee et al., 1986 © 1986 IEEE.)